Finanziato dall'Unione europea NextGenerationEU | Ministero dell'Università e della Ricerca | Italiadomani PIANO NAZIONALE DI RIPRESA E RESILIENZA

multi-Risk sciEnce for resilienT commUnities undeR a changiNg climate

Codice progetto MUR: **PE00000005** – CUP LEAD PARTNER B53C22004020002

Deliverable title: Report the output to TS spokes: identify and select the enablers

Deliverable ID: 2.5.3

Due date: 31/03/2026

Submission date: 27/03/2026

AUTHORS

Silvio Coda (UniNA); Giuseppe Bausilio (UniNA); Diego Di Martire (UniNA); Domenico Calcaterra (UniNA); Lucia Coppola (UniNA); Francesco Silvestri (UniNA); Carlo Esposito (UniRoma1); Leonardo Maria Giannini (UniRoma1); Giacomo Titti (UniBO); Lisa Borgatti (UniBO); Marina Pirulli (PoliTO), Giulia La Porta (PoliTO); Massimiliano Alvioli (CNR IRPI); Ivan Marchesini (CNR IRPI); Massimiliano Melillo (CNR IRPI); Francesca Da Porto (UniPD); Elisa Saler (UniPD)

1. Technical references

Project Acronym	RETURN
Project Title	multi-Risk sciEnce for resilienT commUnities undeR a changiNg climate
Project Coordinator	Domenico Calcaterra UNIVERSITA DEGLI STUDI DI NAPOLI FEDERICO II domcalca@unina.it
Project Duration	December 2022 – November 2025 (36 months)

Deliverable No.	DV2.5.3
Dissemination level*	
Work Package	WP5 - Outcomes for mitigation strategies
Task	T 2.5.3 - Remediation and mitigation solutions in a resilience perspective for other transversal Spokes
Lead beneficiary	UniNA
Contributing beneficiary/ies	UniNA, UniRoma1, UniBO, CNR IRPI, UniPD, PoliTO

* PU = Public

PP = Restricted to other programme participants (including the Commission Services)

RE = Restricted to a group specified by the consortium (including the Commission Services)

CO = Confidential, only for members of the consortium (including the Commission Services)

1.1. Document history

Version	Date	Lead contributor	Description
0.1	13/03/2026	UNINA	First draft
0.2	16/03/2026	VS2 Coordinators	Critical review and proofreading
0.3	xx	xxxx	Edits for approval
0.4	xxxxx	xxx	Final version

2. ABSTRACT

This deliverable reports the results of the operational phase of Task 2.5.3, dedicated to the implementation of the RETURN toolchains for the assessment of Ground Instabilities (GIs) in three Demonstration Cases (DCs): the City of Naples, Calabria DC and Alemagna DC. Building upon the methodological framework defined in previous tasks, the work presented here aims to verify the performance, scalability and operational relevance of the selected tools when applied to real environments characterised by different geomorphological and infrastructural settings, and to translate the resulting modelling outputs into mitigation strategies consistent with the preventive, protective, structural and non-structural categories defined within the RETURN framework.

The adopted toolchains address a wide spectrum of GI types—including anthropogenic sinkholes, shallow landslides, debris flows and rockfalls—through the combined use of physically based, statistical and morphometric models. The workflow includes the assessment of predisposition conditions, preparatory factors, the incorporation of hydrological and seismic triggers, and the construction of Ground Instability scenarios, complemented where appropriate by runout simulations. Applications were conducted at scales ranging from basin-wide to linear-infrastructure corridors, depending on the characteristics of each DC.

The analytical activities benefitted from continuous interaction with the Transversal Spokes TS1 and TS2, which ensured methodological consistency and coherence with the broader RETURN framework. In parallel, stakeholders such as the Gruppo Ferrovie dello Stato (FS) and ANAS contributed by providing datasets, site-specific information and indications on priority areas for the application of the toolchains, thereby reinforcing the operational relevance of the analyses.

The results show that, despite inherent limitations related to data availability and the complexity of the investigated processes, the toolchains generate coherent and spatially explicit outputs suitable for supporting scenario-based decision-making in multi-hazard contexts. The deliverable also outlines the mitigation strategies and real-time monitoring solutions derived from the modelling results, following the taxonomy of preventive, protective, structural and non-structural measures described in DV2.5.1.

Overall, the work demonstrates the applicability of the RETURN toolchains for multi-scale ground-instability assessment and provides indications for future improvements aimed at strengthening their integration into decision-support workflows and stakeholder-driven risk-management processes.

3. Table of contents

3.1. List of Tables

3.2. List of Figures

multi-Risk sciEnce for resilienT commUnities undeR a changiNg climate

Codice progetto MUR: PE00000005 – CUP LEAD PARTNER H93C22000610002

Deliverable title: Complements for multiple hazard scenarios from other vertical Spokes

Deliverable ID: 2.5.2

Due date: 15/03/2026

Submission date: 13/03/2026

AUTHORS

Luca Peruzzo (UNIPD), Giovanni Forte (UNINA), Lucia Mele (UNINA), Valeria Lo Presti (UNIPA), Diego Di Martire (UNINA), Silvio Coda (UNINA), Giorgio Cassiani (UNIPD), Domenico Calcaterra (UNINA), Francesca Bozzano (UNIROMA1), Francesco Silvestri (UNINA), Rosa Colacicco (UNIBA), Marco Bracci (UNIPA), Filippo Zaniboni (UNIBO), Scacchia Elena (ISPRA), Giovanni Poneti (OGS), Silvia Ceramicola (OGS), Daniele Spatola (UNIROMA1), Leonardo Maria Giannini (UNIROMA1), Carlo Esposito (UNIROMA1), Salvatore Martino (UNIROMA1)

4. Introductory Section

4.1. Background

In the framework of the Vertical Spoke 2 (VS2) of the RETURN project, the main objective was the development of operational toolchains, that is, sequences of computational and analytical tools designed to produce scenarios of territorial instability associated with specific types of preparation and triggering processes, each characterized by a given intensity.

On the basis of the developed methodological approach, **Work Package 5 (WP5)** focused on aspects related to mitigation strategies and on interactions with other Spokes and stakeholder partners of the project.

In general, WP5 is structured into the following Tasks:

- **2.5.1** Mitigation solutions with respect to ground instabilities
- **2.5.2** Complements for multiple hazard scenarios from other Vertical Spokes
- **2.5.3** Remediation and mitigation solutions in a resilience perspective for other Transversal Spokes
- **2.5.4** Eco-sustainable mitigation of ground instability scenarios in a changing climate framework

4.2. Introduction

Task 2.5.3, entitled *Remediation and Mitigation Solutions in a Resilience Perspective for Other Transversal Spokes*, focuses on the interactions with the Transversal Spokes (TS) of the RETURN project to assess scenarios of Ground Instabilities (GIs) potentially affecting urban settlements (TS1) and strategic infrastructures (TS2), and to develop mitigation protocols aimed at increasing their resilience.

Within the RETURN project, *toolchains* represent structured logical–operational workflows composed of sequences of computational and analytical tools designed to assess and simulate ground instability scenarios. Each toolchain integrates multiple instruments addressing different stages of the process—ranging from the evaluation of predisposing conditions to the analysis of preparatory and triggering factors, and finally to the simulation of propagation effects. This modular and hierarchical approach enables a coherent and multi-scale representation of the phenomena, where outputs from one analytical stage become inputs for the next, thus ensuring continuity across the modelling chain. The ultimate goal of the toolchains is to generate qualitative, semi-quantitative, and quantitative scenarios capable of describing the spatial and, where possible, temporal evolution of instability processes, supporting both scientific understanding and decision-making in risk mitigation and territorial planning.

In reference to the GIs analyzed within the RETURN project (Table 1), the involvement of stakeholders allowed the identification of sites affected by specific GIs where the methodological approach developed within VS2 could be applied. These sites, referred to as *Demonstration Cases* (DCs), served as the final test bench for the toolchains, aimed at demonstrating their potential to generate scenarios of instability effects expressed in terms of invasion extent, mobilizable volumes, or phenomenon magnitude, both in urban environments and in relation to linear infrastructures. Specifically, three DCs have been analyzed in this deliverable: the City of Naples, Calabria DC, and Alemagna DC. A detailed description of these sites and the applied toolchains is provided in the following section.

In this framework, the definition of mitigation criteria plays a key role in translating the outcomes of instability modeling into practical strategies for risk reduction and resilience enhancement. Mitigation is conceived as a combination of actions targeting the fundamental components of risk—hazard, vulnerability, and exposure—with the objective of reducing the probability of occurrence, the potential damage, or the number and value of exposed elements, depending on the specific territorial and geological context.

For ground instabilities, these strategies are typically distinguished into active (preventive) and passive (protective) measures. The former aim to reduce the likelihood of triggering instability processes by

increasing stabilizing actions or reducing destabilizing ones, acting directly on the causes of the phenomenon. Passive measures, on the other hand, are designed to limit the impact of events that have already been initiated, by controlling, intercepting, or dissipating the energy of the moving mass. Within this category, a particularly relevant role is played by monitoring systems and early warning networks, which represent essential tools for both risk management and emergency preparedness. These systems enable the continuous observation of physical, hydrological, and meteorological parameters, providing real-time data that can be integrated with predictive models to forecast the evolution of instability processes. When properly calibrated and combined with alert protocols, they form the backbone of Early Warning Systems (EWS), allowing timely activation of mitigation or evacuation measures and, consequently, a significant reduction in vulnerability and exposure.

This conceptual framework, further detailed in Deliverable 2.5.1 and summarized in Table 2, provides the foundation for identifying and classifying remedial solutions to be applied within the Demonstration Cases and further discussed in the concluding part of the report.

Table 1 – Typology of Ground Instabilities with indication of the processes analyzed for the Demonstration Cases (modified from DV2.2.3).

GENERAL CLASSIFICATION			
Ground Instabilities	Subaerial Landslides	Subaerial Slow Landslides Typologies	*Slow Flows (Earthflows)*
			Slow Slides (Rotational and planar Slides, Soil slips)
			Slow Spread & Slow Slope Deformations (Spread (except Liquefaction), Rock/Soil Slope Deformations, Creep, DsGSD)
		Subaerial Rapid Landslides Typologies	*Rapid Flows (Debris flows, Mudflows)*
			Rapid Slides (Rock Slides, Rock Avalanches)
			Falls & Topples (Rock Falls, Rock Topples)
	Submarine landslides	Submarine Landslides Typologies	*Canyon head Landslides*
			Inner shelf/Insular shelf Landslides
	Sinkholes	Slow Sinkholes Typologies	*Slow Sinkholes (All Types)*
		Rapid Sinkholes Typologies	*Rapid Sinkholes (All types)*
	Subsidence	Subsidence Typologies	*Subsidence (All types)*
	Liquefaction	Liquefaction Typologies	*Liquefaction (All types)*

Table 2 - Classification of Active/Preventive Remedial Measures, as reported in DV 2.5.1.

Principle	Method	Execution		Soils / Rocks
Increase in stabilyzing forces	Increase in normal stress	Backfilling and toe protection works	SN	Landslides
	Increase in shear strength	Thermal stabilization	SN	Liquefaction
		Injections	SN	Sinkhole
		Increase in density	SN	SI = Structural Invasive
		Adjustement of grain size distribution (replacement or mixing)	SN	SN = Structural Non-invasive
		Reinforced soils	SI	
	Reduction in positive pore water pressure (increase in suction)	Drainage	SI	NS = Non-Structural
		Electro-osmosis	SN	
		Induced Partial Saturation (IPS)	SN	
Decrease in instabilyzing forces	Reduction in shear forces along the slip surface	Unloading excavation at the crest of the slope	SN	
		Slope reshaping	SN	
	Tangential stress transfer to structural elements or stable formations	Retaining and diaphragm walls	SI	
		Soil nails	SI	
		Anchors	SI	
		Piles	SI	

This document is organized as follows:

Section 5 describes the Demonstration Cases and the adopted toolchains, including the interactions with the Transversal Spokes and stakeholder partners, as well as a detailed overview of each Demonstration Case and the corresponding toolchain applied.

Section 6 illustrates the application of the toolchains to the selected sites, presenting the main results obtained for each case.

Section 7 focuses on the definition of protocols for Ground Instability mitigation, discussing the proposed mitigation strategies, their application within the Demonstration Cases, and the integration of real-time monitoring and early warning systems.

Finally, Section 8 summarizes the main conclusions and outlines perspectives for future developments.

5. Demonstration Cases and Toolchains

5.1. Interaction with Transversal Spokes and Stakeholders

Within the RETURN project, continuous intra- and inter-spoke collaboration has characterized the different phases of the workflow. A particularly representative example of this interaction was the application of the methodological tool-chained approach developed by VS2 for producing GI scenarios in terms of quantification of the phenomena and their effects. Specifically, several stakeholders—partners of the project—provided Demonstration Cases (DCs; Fig. 1) in which the methodology was practically tested. Their analysis was carried out within VS2 and in collaboration with the Transversal Spokes (TSs) to evaluate the effects of GIs on the urban environment (TS1) and on linear infrastructures (TS2). Moreover, part of the analysis was performed in the framework of External Calls of RETURN project.

The following sections describe the DCs analyzed in collaboration with TS1 and TS2, with reference to the type of GI, the stakeholders involved, and the related toolchains adopted.

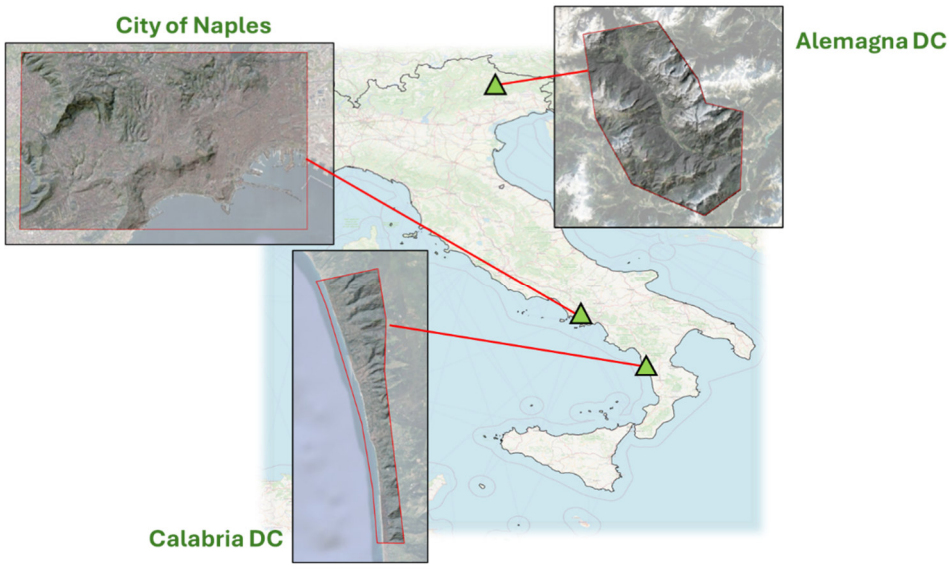

Figure 1 – Location of the Demonstration Cases (DCs).

5.1.1. City of Naples Demonstration Case

General description

The City of Naples Demonstration Case (Fig. 2a) encompasses the urban area of Naples and the surrounding hilly sectors, with particular attention to Camaldoli Hill, the highest relief within the urban territory and one of the most active areas in terms of rainfall-induced shallow landslides. The city, built on a thick and heterogeneous volcanic substrate and affected by centuries of intense human modification, represents a highly complex environment where both debris-flow processes along the volcanic slopes and anthropogenic sinkholes within the urban fabric occur frequently and can produce significant damage.

Geological and geomorphological setting

The geological structure of the Demonstration Case is controlled by the Phlegraean Fields volcanic district, an active caldera system whose explosive history has shaped the morphology and subsoil of Naples. The area is characterized by extensive deposits derived from the major eruptions of the Campanian Ignimbrite (CI – 39ky; De Vivo et al., 2001) and the Neapolitan Yellow Tuff (NYT – 15ky; Scarpati et al., 2012), whose distribution and internal architecture are illustrated in Fig. 2b. These units form the main structural framework of the city: the Campanian Ignimbrite provides a welded, locally massive substratum, while the NYT constitutes a variably welded, porous and heavily fractured bedrock whose mechanical properties influence both slope stability and the behavior of underground cavities (Tufano et al., 2022).

Above the tuff bedrock, the slopes of Camaldoli Hill and neighbouring reliefs are mantled by a thick sequence of unconsolidated volcaniclastic deposits, including ash-fall layers, pumiceous horizons, paleosols and reworked pyroclastic material. Their spatial variability, combined with steep slope gradients and the presence of relatively impermeable buried paleosols, favours the initiation of shallow failures and flow-like movements during intense rainfall events. Numerous studies conducted over the past decades have documented the high propensity of these volcaniclastic covers to undergo rapid mobilisation, especially when the upper ash-pumice horizons become saturated and pore-water pressures increase (Calcaterra et al., 2007; Fusco et al., 2023, 2019). The resulting debris-flow phenomena are widely represented in the landslide inventory (Fig. 2c).

The geomorphological setting of the urban area is further complicated by a long history of anthropogenic modification. Extensive underground quarrying of the NYT, the presence of abandoned cavities, leaking drainage systems and thick anthropogenic fills create conditions conducive to sinkhole development. These phenomena, largely concentrated in densely urbanised districts, involve sudden collapses of the ground surface due to cavity-roof failures or subsurface erosion processes. Recent investigations highlight the increasing frequency of such events across Naples, emphasising the role of subsurface water circulation, structural degradation and the intrinsic fragility of the volcanic substrate (Tufano et al., 2022). Examples of sinkhole collapses are shown in Fig. 2d.

Overall, the interplay between volcanic stratigraphy, steep pyroclastic-mantled slopes, hydrological sensitivity of the volcaniclastic covers and widespread anthropogenic modifications results in a geomorphological system highly susceptible to both debris-flow processes and anthropogenic sinkholes.

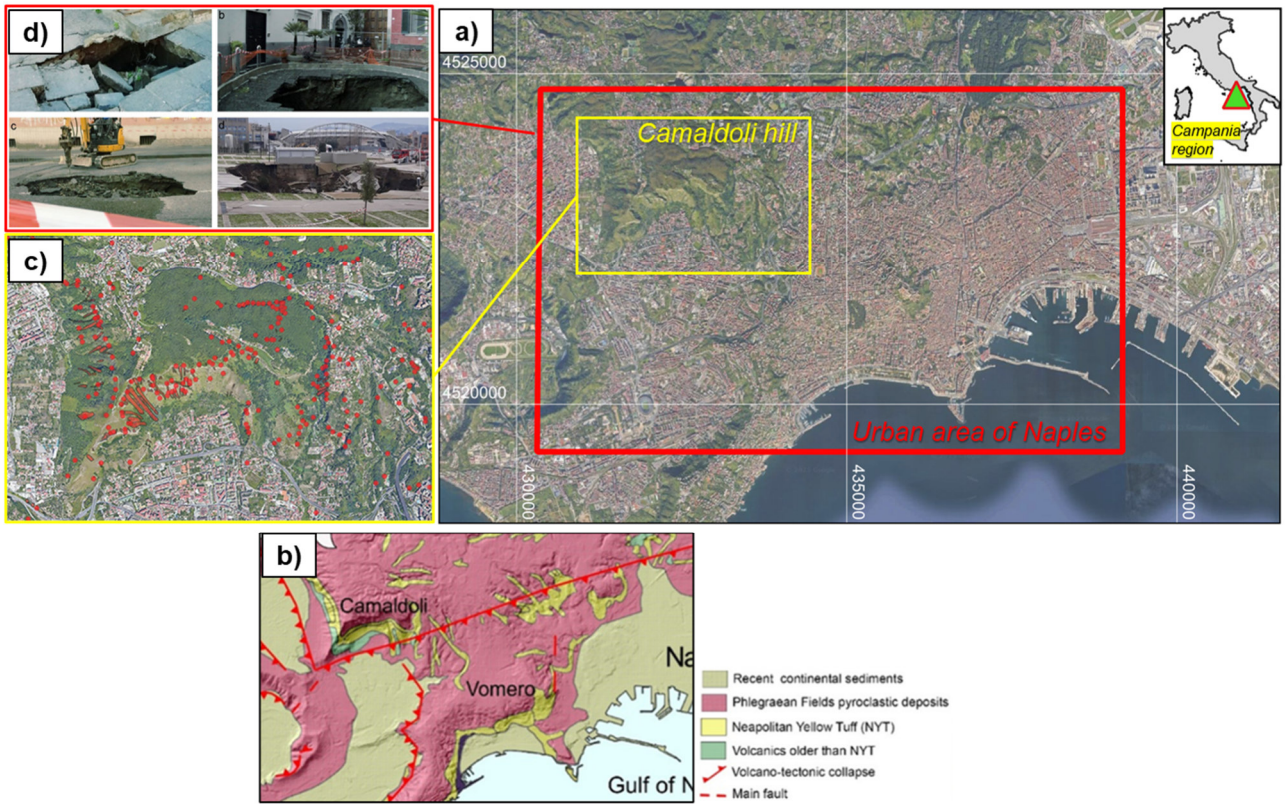

Figure 2 - a) City of Naples DC; b) Geological map (from Tufano et al., 2022); c) Landslide inventory of Camaldoli hill (Fusco et al., 2023); c) Example of anthropogenic sinkholes in the urban area of Naples (Tufano et al., 2022).

Types of GI analyzed

The City of Naples Demonstration Case focuses on two types of gravitational processes particularly relevant within the study area:

- Debris-flow and shallow flow-like landslides affecting the volcanic slopes of Camaldoli Hill and adjacent reliefs;
- Anthropogenic sinkholes occurring within the urban area, primarily associated with cavity collapse and subsurface erosion.

Spokes and stakeholders involved

The activities in the City of Naples Demonstration Case involve the TS1 Spoke.

5.1.2. Calabria Demonstration Case

General description

The Calabria Demonstration Case is located along the Tyrrhenian coastal sector of the northern Calabria region (southern Italy), extending between the municipalities of Fuscaldo, Paola, San Lucido and Falconara Albanese (Fig. 3a). The area includes a strategic section of the national railway corridor running parallel to the coastline at the foot of the Coastal Range, where steep, tectonically controlled slopes host recurrent gravitational instabilities. The study domain is characterised by narrow coastal plains, deeply incised catchments, and steeply rising reliefs where slope gradients locally exceed 35–40°.

Geological and geomorphological setting

From a geological standpoint, the DC lies on the western flank of the Coastal Range, a morphostructural high belonging to the broader Calabria–Peloritani terrane (Bonardi et al., 2001). This crystalline-metamorphic massif consists of a complex pile of nappes including Variscan and pre-Variscan basement units, overlain by remnants of Mesozoic to Cenozoic sedimentary covers. The structural architecture has been profoundly shaped by Miocene–Quaternary tectonics, which controlled both regional uplift and the development of major fault systems.

Recent detailed mapping and structural analyses in the central sector of the Coastal Range highlight the occurrence of stacked ophiolitic and continental crust units affected by Alpine HP–LT metamorphism and later extensional deformation (Filice et al., 2015). These findings confirm the strongly composite and anisotropic nature of the metamorphic basement that characterises the steep slopes above the coastal corridor. Along the Tyrrhenian margin, the Coastal Range is bounded by steep, linear mountain fronts associated with N–NNW-trending normal faults, which have accommodated significant Plio–Quaternary uplift (Robustelli et al., 2005 and references therein). Uplift rates ranging between 0.5 and 1 mm/yr are reported for this sector and are reflected in the widespread presence of marine terraces and hanging alluvial surfaces.

The landscape is strongly controlled by tectonics, as highlighted by the low mountain-front sinuosity and the presence of high-angle normal fault scarps (Sorriso-Valvo and Sylvester, 1993). These long-term uplift processes favoured the incision of narrow, V-shaped valleys that feed a system of Late Pleistocene alluvial fans and coalescent fan complexes (Robustelli et al., 2005). The piedmont zone, where the railway infrastructure is located, is therefore an interface between actively uplifting mountain slopes and coastal sedimentary systems sensitive to both marine and alluvial processes. The crystalline bedrock, typically consisting of gneiss, schists, granitoids and metabasites (Bonardi et al., 2001), is locally overlain by Miocene sedimentary successions and by Quaternary deposits. Steep slopes developed on these lithologies provide favourable conditions for rockfalls, topples and debris flows, especially where weathering profiles or tectonic discontinuities reduce rock mass strength.

Types of GIs analyzed

Given the geomorphological and litho-structural configuration, the Calabria Demonstration Case focuses mainly on:

- Rockfall processes along the steep bedrock slopes above the railway line;
- Debris flows and rapid flow-like phenomena originating in small, deeply incised catchments that drain directly toward the coastal plain (Fig. 3c).

These gravitational processes are consistent with the dominant sedimentary and erosive dynamics observed along the Coastal Range (Sorriso-Valvo & Sylvester, 1993; Robustelli et al., 2005), where slope instability represents a natural response to active uplift and rapid incision.

Spokes and stakeholders involved

The activities carried out in this Demonstration Case involve the TS2 Spoke and Gruppo Ferrovie dello Stato (FS).

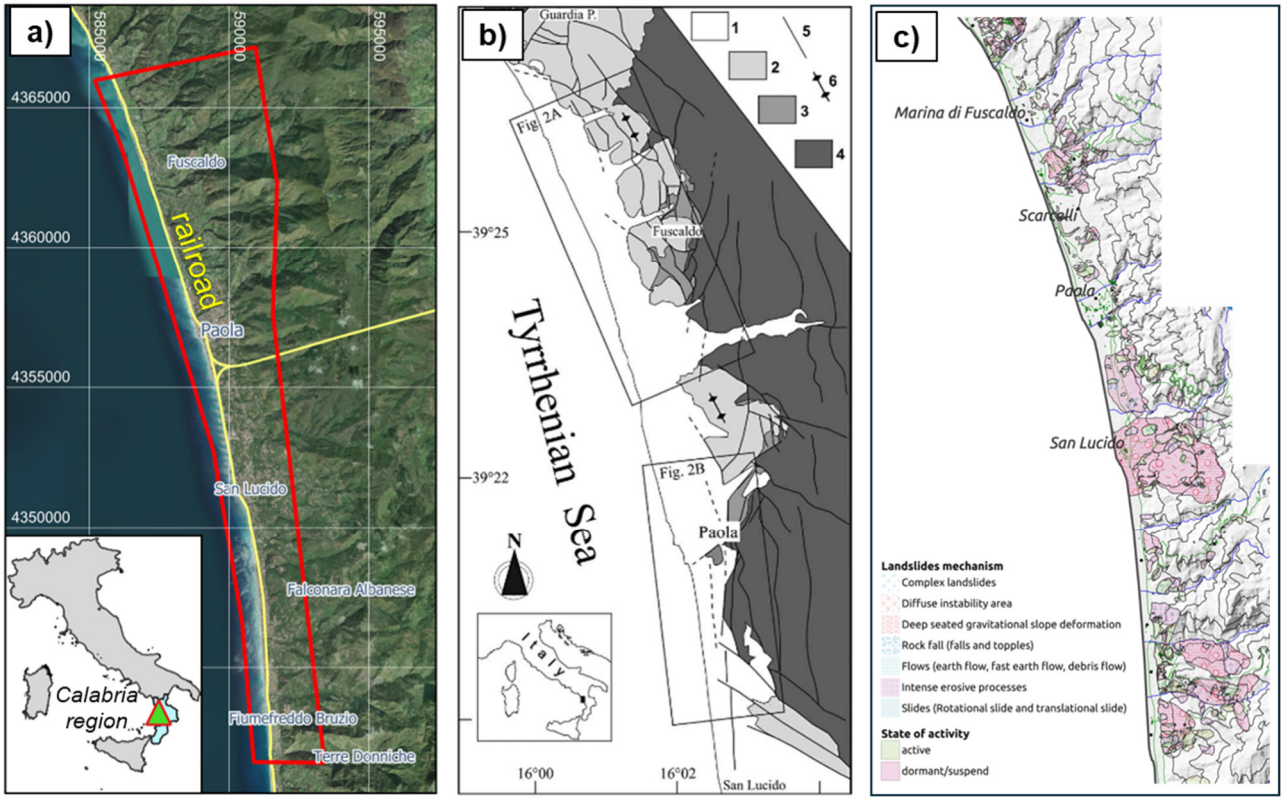

Figure 3 - a) Calabria DC; b) Geological map of the study area (from Robustelli et al., 2005): (1) Quaternary to Recent deposits; (2) calcarenites and clays (Upper Miocene); (3) conglomerates and sandstones (Upper Miocene); (4) crystalline-metamorphyic bedrock (Paleozoic); (5) faults; (6) fold axes. c) Landslide inventory (Cianflone et al., 2025).

5.1.3. Alemagna Demonstration Case

General description

The Alemagna Demonstration Case is located in the northern Veneto Region (north-eastern Italy), encompassing the upper Boite Valley and the surrounding Dolomite massifs between Cortina d'Ampezzo, San Vito di Cadore, Borca di Cadore, Valle di Cadore, Zoppè di Cadore and Fornesighe (Fig. 4a). The area hosts a section of the Strada Statale 51 "Alemagna" (SS51), an important north–south road link connecting the Cadore region to the Veneto plain. The combination of steep alpine slopes, narrow valley floors and extensive unconsolidated deposits results in a highly dynamic geomorphological setting (Fig. 4b) where multiple gravitational processes interact with the territorial infrastructure.

Geological and geomorphological setting

Geologically, Alemagna area belongs to the eastern Dolomites, characterised by Mesozoic carbonate platforms and basinal successions that were deformed during Alpine Orogeny. The stratigraphic framework includes extensive Triassic dolostones, limestones and marly formations, forming massive rock walls, stepped slopes and narrow incised valleys, as described in the Carta Geologica d'Italia – Foglio 029 Cortina d'Ampezzo (ISPRA, 2007). These lithologies are dissected by a complex system of thrusts and high-angle faults (Fig. 4c), which exert significant control on slope geometry, rock fracturing and the spatial distribution of gravitational processes.

The area has been profoundly shaped by Quaternary glacial and periglacial dynamics, responsible for carving U-shaped valleys, hanging basins and over-steepened lateral slopes. Thick accumulations of glacial and paraglacial debris, colluvium, rockfall material and avalanche deposits mantle the valley sides and floors, providing abundant source material for rapid mass movements.

This morphological legacy, combined with present-day climatic forcing, underlies the long-term activity of slope instabilities documented by geomorphological studies in the region (Borgatti and Soldati, 2010; Panizza et al., 1996). Among the dominant processes, debris flows are particularly significant. Active channels such as Cancia—extensively analysed in Deganutti and Tecca (2013)—demonstrate the ability of small high-relief catchments to produce frequent and highly mobile flows. However, the region is also characterised by widespread rockfalls, rotational and translational slides, and complex landslides, as shown in the IFFI inventory (Fig. 4d). Their distribution reflects lithological contrasts, structural controls and inherited glacial morphology.

Overall, the interplay between steep structural slopes, fractured carbonate bedrock and glacially conditioned deposits creates a geomorphological system highly susceptible to rapid mass movements, with debris flows playing a central role in the hazard context of the DC.

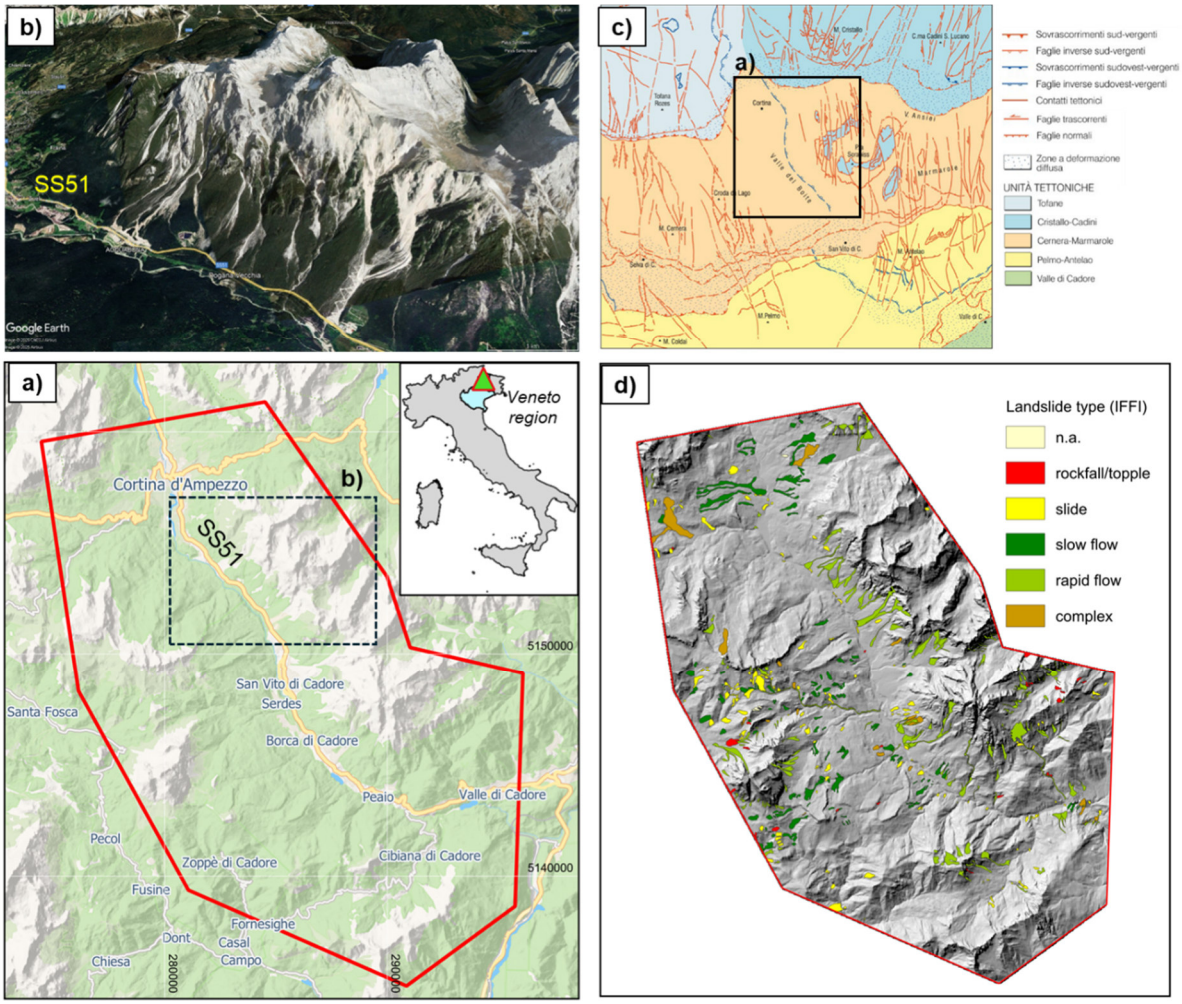

Figure 4 - a) Alemagna DC; b) prospective view of the eastern reliefs (satellite image from Google Earth); c) Regional tectonic scheme (ISPRA, 2007); d) Landslide inventory (IFFI Project).

Type of GI analyzed

Although various gravitational processes are present across the DC, including rockfalls, slides and complex movements (Fig. 4d), it specifically focuses on debris-flow phenomena, which are among the most recurrent and hazardous processes in the upper Boite Valley. Debris flows typically originate in steep,

debris-filled headwater basins and propagate along confined channels towards valley-floor fans and conoids.

Spokes and stakeholders involved

The activities within the DC involve TS2 Spoke and ANAS S.p.A.

5.2. Adopted Toolchains

Among the toolchains developed by VS2 (described in detail into DVs 2.4.4 and 2.4.6), three were applied to the DCs (Rockfall and Slope Failures, Soil Shallow Slides, and Anthropogenic Sinkholes). Table 3 reports the tools used in each toolchain for producing GI scenarios in the DCs. All the developed tools have been implemented in the ARGUS platform (Analysis of multihazaRds from GroUnd instabilities Scenarios), in the framework of the ALICE External Call Project of VS2 Spoke.

Table 3 - Tools and toolchains adopted for analyzing the DCs of this deliverable (modified from DVs 2.4.4 and 2.4.6).

GI TYPE	KINEMATICS	SCALE	PREDISPOSITION	PREPARATION	FAILURE / TRIGGERING	RUNOUT / EFFECT
Anthropogenic Sinkholes	Rapid	Basin to regional	KATABASIS	-	-	Magnitude (diameter scenarios)
Rockfall/topple	Rapid	Local to regional	Multiple threshold approach	-	-	STONE (trajectory count)
Shallow soil slides_2 (debris/mud avalanche/flows)	Rapid	Basin to regional	Parsifal_T_dry WP2 Box	Wildfire TOPMODEL RU scenarios	Parsifal_T_s Parsifal_T_r	FoS Volume estimation RASH3D

5.2.1. Toolchain 1. Sinkholes

The toolchain developed for anthropogenic sinkhole analysis has been applied to the urban area of Naples DC. It provides a reproducible framework for assessing the spatial occurrence of sinkholes and their magnitude, expressed through the sinkhole diameter. The methodology is grounded in a statistical and machine-learning-based approach designed to support Task 2.4.3 of WP4 by producing susceptibility maps capable of capturing the interaction between predisposing factors and sinkhole attributes. Unlike karst-related processes, anthropogenic sinkholes form through the collapse of man-made or man-modified underground cavities originating from historical quarrying, abandoned hypogeal structures, piping phenomena, leaking utilities or instability in artificial fills (Guarino and Nisio, 2012; Parise, 2015). These characteristics make presence-only and presence-background modelling strategies particularly suitable for this type of hazard.

Predisposition

The core of the toolchain is an ensemble susceptibility modelling system—named KATABASIS—implemented using Python (version 3.12.11) and GDAL, which combines three algorithms widely applied in spatial prediction problems: Gradient Boosting Machine (GBM) (Friedman, 2001), Random Forest (RF) (Breiman, 2001), and Generalized Linear Model (Nelder and Wedderburn, 1972). The ensemble approach ensures robust performance by merging multiple single-model outputs, each trained on different subsets of pseudo-absence or background points and validated through k-fold cross-validation. Only models exceeding a user-defined ROC threshold (EM_th) are retained. The final ensemble map is generated by a weighted mean in which weights correspond to ROC performance, ensuring that better-performing models have proportionally greater influence.

A fundamental element of the workflow is the definition of predisposing factors, representing geological, geomorphological, hydrological and anthropogenic conditions contributing to collapse susceptibility. These variables are provided as raster layers in *.tif* format with identical extent and resolution.

Before model training, the toolchain performs a Variance Inflation Factor (VIF) analysis to detect multicollinearity among predictors (James et al., 2021). Layers exceeding the VIF threshold are automatically excluded to ensure numerical stability and model interpretability. When no collinearity is detected, the full set of predictors is retained.

GI scenario

The toolchain requires an anthropogenic sinkhole inventory providing the positional information of each recorded event. When the objective is to integrate magnitude, the inventory must also include sinkhole diameter or depth— depending on the scope of the analysis and the available data—which is used as a proxy for event severity because they are directly measurable and correlates with potential damage. As with any statistical learning workflow, inventory completeness critically influences the robustness of the model outputs.

For each machine-learning algorithm, the toolchain generates multiple single models by combining different pseudo-absence/background sets with k-fold cross-validation. The resulting models, each statistically independent due to variations in sampling, are then aggregated into the final ensemble susceptibility raster through performance-based weighting.

The toolchain generates an extensive suite of diagnostic and cartographic products, including VIF barplots, presence/pseudo-absence distribution maps, single-model prediction rasters, the final ensemble susceptibility map, response curves, variable importance diagrams, and performance statistics such as ROC/AUC, Sensitivity, Specificity and standardised True Skill Statistic (sTSS) (Fawcett, 2006). The ensemble susceptibility raster is finally classified into five classes using the Natural Breaks (Jenks) method, accompanied by a histogram representing class area distribution.

When the magnitude-based mode is activated, the sinkhole inventory is partitioned into three magnitude classes, defined by user-specified thresholds in the configuration file. Each class undergoes an independent ensemble modelling workflow, producing three susceptibility maps corresponding to different expected collapse severities. These outputs highlight whether specific areas are more susceptible to larger or smaller sinkhole events, providing scale-dependent insights into potential impacts.

Overall, this toolchain offers a flexible, reproducible and fully customisable statistical framework for anthropogenic sinkhole susceptibility assessment, capable of incorporating event magnitude and a wide range of predisposing factors. Thanks to the integration of multiple algorithms and rigorous cross-validation procedures, it ensures robust performance and is particularly effective in contexts where underground anthropogenic cavities or buried infrastructure exert a primary control on ground instability.

5.2.2. Toolchain 2. Rockfall and Topple Failures

The toolchain for rockfall and topple instability types was applied to the Calabria Demonstration Case at scales ranging from local to regional for rockfall scenarios, considering grid cells as the mapping/analysis unit in the former, and slope units (generated ad hoc or retrieved from a dedicated repository) in the latter.

The first conceptualization of the methodology involved applying machine learning or statistical approaches to assess predisposition to failure (DV2.4.4). In the Calabria DC, however, the available occurrence data derived from landslide inventories (Fig. 3c; Cianflone et al., 2025) are limited in number and mostly refer to areas surrounding urban centers. As a result, they are spatially incomplete and insufficient both for training Spatial Distribution Models (SDMs) and for applying statistical methods, being distributed mainly along the coastal belt while absent in higher-elevation areas.

Given these limitations, a morphological approach was therefore adopted to identify potential rockfall detachment areas, relying on a multiple-threshold morphometric procedure. This solution compensates for the spatial incompleteness of the available occurrence data and allows the extraction of potential source zones directly from the terrain morphology.

In this framework, several morphometric descriptors were computed from the high-resolution LiDAR-derived DTM (2×2 m resolution), including slope, profile curvature, tangential curvature, and local relief. Similar semi-empirical approaches have been successfully applied in previous studies aimed at delimiting rockfall source areas (e.g., Alvioli et al., 2022; Pokharel et al., 2023; Santangelo et al., 2019). Slope was calculated on a 3×3 moving window, while profile and tangential curvatures were obtained using the r.slope.aspect module in GRASS GIS (Hofierka et al., 2009). Local relief was derived on a 5×5 moving window to highlight abrupt discontinuities and areas characterized by significant elevation contrasts.

Different combinations of thresholds were tested and inspected, and the final configuration was selected based on empirical evaluation and expert interpretation. The adopted criteria were:

slope > 60°, relief > 12.7 m, profile curvature > 0.02 m^{-1}, and tangential curvature > 0.04 m^{-1}.

Grid cells simultaneously exceeding all these thresholds were classified as potential rockfall detachment areas.

The subsequent step of the workflow consisted of performing three-dimensional rockfall simulations with the STONE model (Guzzetti et al., 2002), using the previously identified source areas as detachment points. The STONE model is a physically based tool designed to simulate rockfall motion in three dimensions. It requires five main input layers: a digital elevation model (DEM or high-resolution DTM), three raster maps describing the terrain parameters governing energy dissipation during impacts (normal restitution, tangential restitution, and rolling friction), and a raster map of rockfall source cells from which trajectories are initiated. For each source cell, STONE generates multiple trajectories that differ from one another due to random sampling of detachment angles and terrain parameters. These parameters are extracted from Gaussian distributions centered on lithology-dependent values, ensuring a realistic representation of variability in block–ground interactions. The number of simulated trajectories originating from each source cell is proportional to the assigned source probability value, which guarantees adequate sampling in areas characterized by steep slopes and a high likelihood of block release. During propagation, STONE tracks the full three-dimensional path of each block, accounting for bouncing, rolling, energy loss, and runout distance. The model outputs a raster map in which each cell stores the number of simulated trajectories crossing that location, providing a spatially distributed estimate of potential rockfall exposure.

This physically based modelling framework allows consistent simulation over wide areas while maintaining high detail when applied to fine-resolution DTMs, supporting subsequent stages of hazard and impact assessment.

The application of this toolchain derived from the HySTC (Hydrology and Stability of slopes along Transport Corridors) External Call Project of TS2 Spoke.

5.2.3. Toolchain 3. Soil Shallow Slides

The tools composing this toolchain are described in detail in DV2.4.4; here the operational chain is summarised with reference solely to the components effectively employed within the Demonstration Cases (Tab. 3), specifically in the Camaldoli hill of Naples, in Fuscaldo area of the Calabria DC, and in the Alemagna DC. The toolchain addresses the analysis of shallow soil slides and rapid flow-like movements (debris avalanches and debris flows) at scales ranging from the catchment to the regional level. Its structure integrates two alternative approaches for assessing slope predisposition—one physically based and one data-driven—followed, when applicable, by triggering analysis and by scenario modelling for estimating unstable areas, potential volumes and runout distances.

Predisposition

A first method for evaluating predisposition relies on Parsifal_T_dry, a physically based stability model included in *Parsifal_T* toolset (Esposito et al., 2016) that computes the Factor of Safety (FoS) in “dry” conditions, i.e., without the influence of hydrological or seismic perturbations. This module incorporates the spatial configuration of soil thickness, material strength parameters, local slope geometry and geotechnical unit properties to derive a static stability field over the study area. Its formulation makes it suitable for basin to regional applications, provided that the required geotechnical, geometrical and stratigraphic inputs are available or can be reconstructed through geomorphological inference.

As an alternative, predisposition can be evaluated using WP2 Box tool. It has been developed by WP2 of VS2 Spoke (DV2.2.5), and the tool consists of a collection of algorithms for susceptibility analysis based on data-driven models, i.e., Logistic Regression, Weight of Evidence (Van Westen, 1993), and Random Forest (Breiman, 2001). Starting from occurrence or presence data, landslide susceptibility analysis aims to identify areas that are intrinsically prone to slope failures and related processes, based on the spatial distribution of controlling factors. Unlike Parsifal, WP2 Box does not incorporate any preparatory hydrological modelling or triggering component, and its output is strictly a spatial susceptibility representation. When this approach is adopted, subsequent scenario analysis relies directly on the susceptibility results, without transitioning through FoS-based stages.

Preparation and failure

Triggering analysis is performed only when the Parsifal branch of the toolchain is used. For rainfall-induced failures, triggering conditions are derived from the FOCA rainfall database (Claps et al., 2024), which provides long-term records of event-based precipitation. These rainfall inputs are transformed into hydrological forcing through TOPMODEL—a variable contributing area model originally introduced by (Beven et al., 1995)—which estimates the RU index, defined as the ratio between the saturated soil thickness and the total soil thickness. This index expresses the degree of saturation in the soil mantle and serves as the primary hydrological control incorporated into Parsifal_T_wet, which computes the stability field under rainfall-triggered conditions. When required, this hydrological modelling step can be bypassed by adopting predefined RU scenarios to explore a range of possible triggering intensities. For seismic triggering, the module Parsifal_T_s is applied, incorporating earthquake ground-shaking effects into the FoS computation and thus identifying areas expected to reach instability thresholds during seismic events. Additionally, the effect of wildfire events can be considered in the analysis as preparatory factor, specifically introducing a reduction in cohesion for the burned areas based on soil and vegetation characteristics, according to a similar approach used by Ferrarotti (2026).

GI scenarios

In configurations where failure is modelled through Parsifal, the triggering modules yield FoS maps describing stability conditions under rainfall or seismic forcing. Areas where the Factor of Safety falls below unity are classified as potentially unstable and form the basis for scenario building. In contrast, when susceptibility is obtained through WP2 Box, no FoS computation and runout modelling are performed.

Scenario development integrates stability or susceptibility outcomes with estimations of potential failure volumes and runout propagation. When Parsifal is used, a morphological volume estimation procedure is applied to areas where FoS < 1, providing an approximate order of magnitude for the volumes susceptible to mobilisation. Conversely, when WP2 Box is employed, volume estimation is carried out for the areas characterized by the highest susceptibility classes. In both branches, runout modelling is performed using RASH3D (Pirulli et al., 2007), applied to selected catchments of interest. This tool allows simulating the propagation phase of rapid flow-like movements, such as debris flows originating from rainfall-induced shallow landslide failures, thus delineating potential impacted areas. For the Parsifal-based workflow, the source areas correspond to zones exhibiting FoS < 1 under the selected triggering condition.

Overall, Toolchain 3 provides a flexible and modular framework capable of supporting different data contexts and analytical objectives. The two predisposition approaches—physically based FoS modelling and machine-learning-based susceptibility mapping—can be used alternatively depending on data availability and the desired level of physical detail. Triggering analysis and scenario development modules allow extending predisposition assessments into dynamic scenarios that incorporate rainfall or seismic forcing and provide first-order estimations of volumes and runout. This structure ensures methodological consistency while allowing adaptation to the specific needs and datasets of the Demonstration Cases.

A resume of the tools adopted for each DC is reported in Tab. 4.

Table 4 - Approaches and tools adopted for the Toolchain 3 in the DCs.

DC	PREDISPOSITION	PREPARATION	FAILURE	RUNOUT / effect
City of Naples	Parsifal_T_dry	RU scenarios Burned areas	Parsifal_T_s Parsifal_T_r	Volume estimation
Calabria	Parsifal_T_dry	TOPMODEL	Parsifal_T_s Parsifal_T_r	Volume estimation RASH3D
Alemagna	WP2 Box	-	-	-

6. Application of the Toolchains

6.1. Sinkholes and debris flows in the metropolitan area of Naples

Sinkholes – Predisposition

As stated in Section 5.2.1, the quality and the amount of information contained in an inventory is a crucial element of any statistical analysis. In this case, the training phase of the Anthropogenic Sinkhole Analysis has been carried out for the entire municipality, as a smaller area would have conducted errors during the modeling phase.

Regarding the Predisposing factors, a total of 22 rasters were selected and used for the analysis:

- AS_Net_Den, density of aqueduct and sewer main pipelines network;
- AS_Net_Dis, distance to aqueduct and sewer main pipelines network;
- Aspect;
- Cav_Den, density of underground man-made cavities;
- Cav_Dis, distance to underground man-made cavities;
- Cov_Thic, thickness of the cover layer;
- DTM, the Digital Terrain Model;
- EGMS_E, the West-East component of the interferometric data from 2018 to 2022;
- EGMS_U, the vertical component of the interferometric data from 2018 to 2022;
- Geology;
- GW_Level, water table level;
- Hydr_Den, density of the Hydrographic Network;
- Hydr_Dis, distance to the Hydrographic Network;
- Land_Use;
- M_YRain, average annual rainfall;
- Plan_Cur, Planar Curvature;
- Prof_Cur, Profile Curvature;
- Road_Den, road network density to simulate the secondary aqueduct and sewer network;
- Road_Dis, distance to road network to simulate the secondary aqueduct and sewer network;
- Slope, the slope angle;
- TPI, Topographic Position Index;
- TWI, Topographic Wetness Index.

The VIF Analysis highlighted some collinearity problems with some predisposing factors (Fig. 5a). EGMS_E and EGMS_U are characterized by huge VIF values (respectively 10.51 and 9.51), this was expected due to the uplifting activity of the Phlegrean Volcanic Field that heavily impact the western sector of the city of Naples. The other critical values are related to the DTM (5.54) and GW_Lev (5.17). This is mostly caused by the presence of multiple predisposing factors derived from the DTM itself (Aspect, Slop, Planar and Profile Curvature, etc.). After removing from the Analysis both EGMS_E and DTM, there seems to be no more collinearity problems (Fig. 5b).

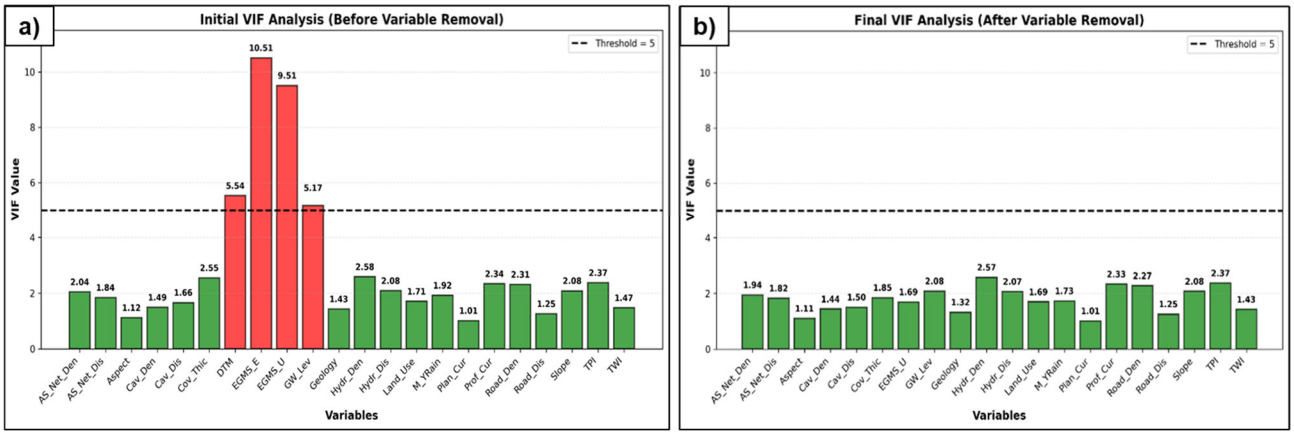

Figure 5 - Results of the a) first and b) final VIF analysis.

Following the VIF Analysis, the sinkhole inventory has been divided into three magnitude sub-sets. In this case, the analysis is based on the sinkhole diameter, as it was the most available data. The sinkhole inventory was divided into:

- Group 1, 43 sinkholes with diameter size of maximum 1 meter, divided into 30 training data and 13 test data;
- Group 2, 62 sinkholes with diameter size between 1 meter and 3 meters, divided into 43 training data and 19 test data;
- Group 3, 57 sinkholes with diameter bigger than 3 meters, divided into 39 training data and 18 test data.

The following analysis produced a total of 45 anthropogenic sinkhole susceptibility maps per Group (Group 1 – Fig. 6a; Group 2 – Fig. 6b; Group 3 – Fig. 6c).

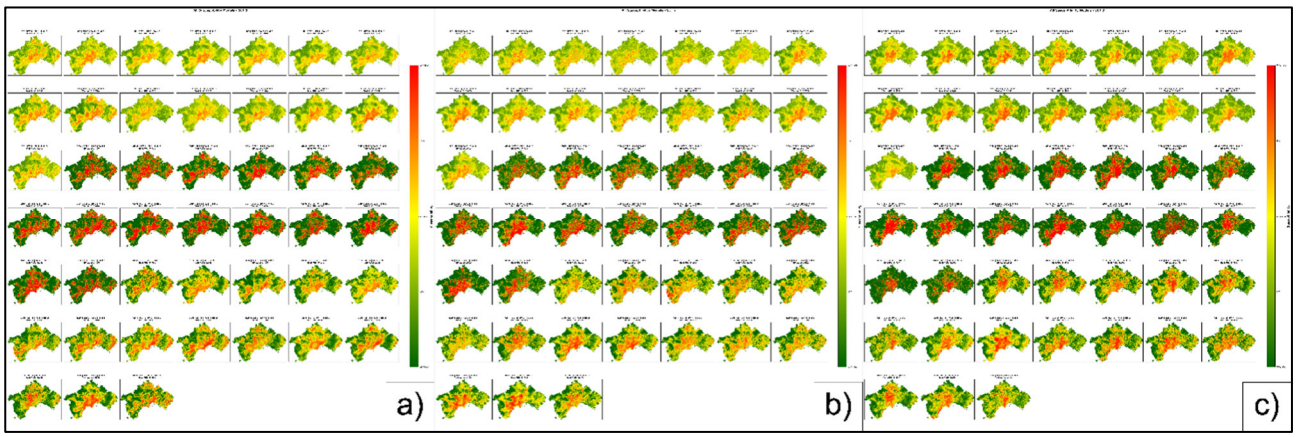

Figure 6 - The 135 models produced for this analysis. a) Group 1; b) Group 2; c) Group 3.

Out of the 135 models, 4 models (2 GBM and 2 GLM) for Group 1, 3 models (1 GBM and 2 GLM) for Group 2, and 1 RF model for Group 3 did not reach the minimum threshold (ROC score = 0.70) needed to be implemented in the ensembled model. From the Variance Importance Analysis (an example for Group 1 is reported in Fig. 7), the distance to the main Aqueduct and Sewer network, the distance to the rain network and the distance to the underground man-made cavities seem to be the most important predisposing factors.

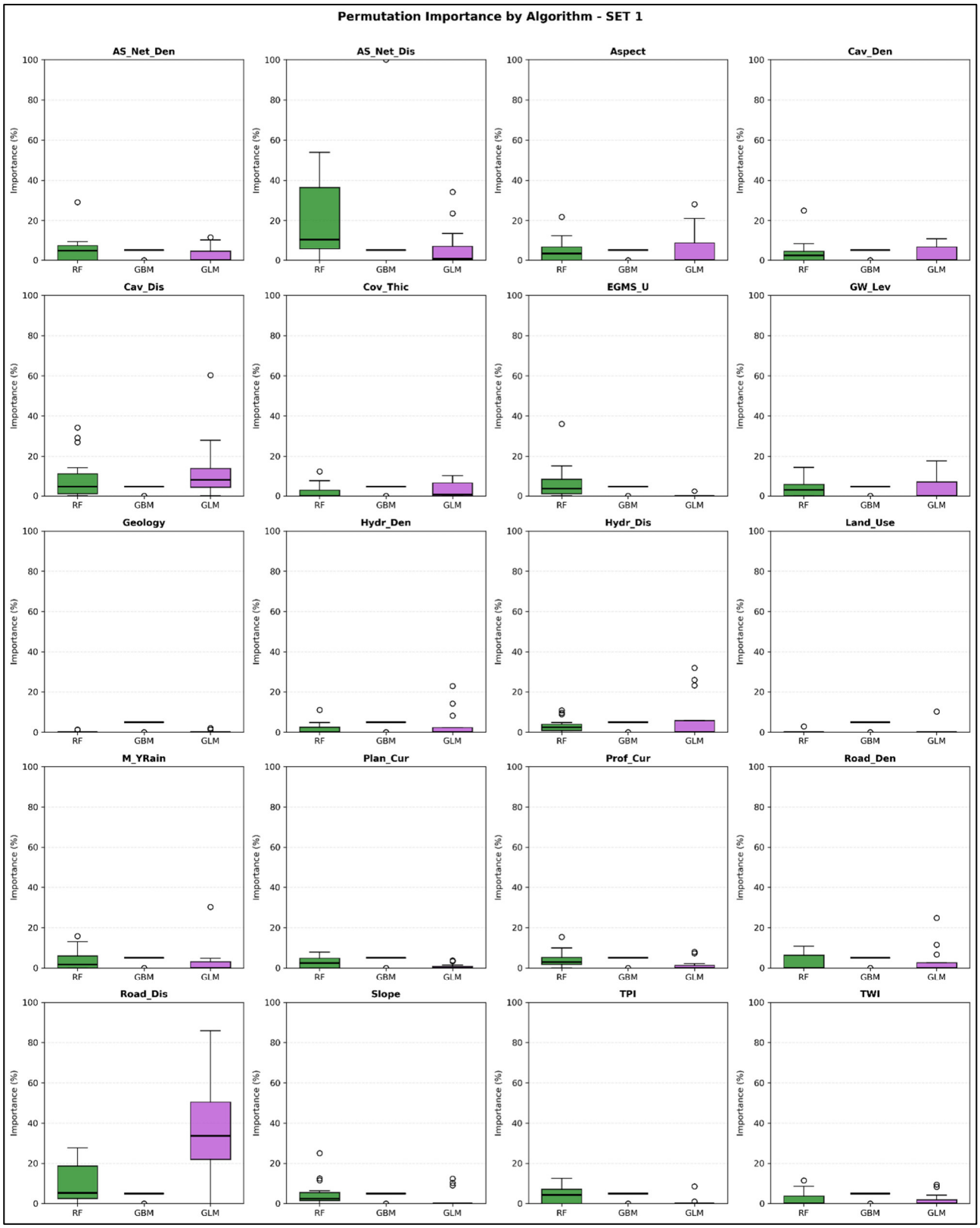

Figure 7 – Predisposing Factor importance for Group 1.

Regarding the response curves (an example for Group 1 is reported in Fig. 8), they show a similar trend for all three groups, with increasing susceptibility with higher values of aqueduct, sewer, road, and cavities networks density, and decreasing response with the increase of the distance to the aforementioned networks. Other predisposing factors show a weak response, except for hydrographic network density that shows a decreasing trend towards higher density.

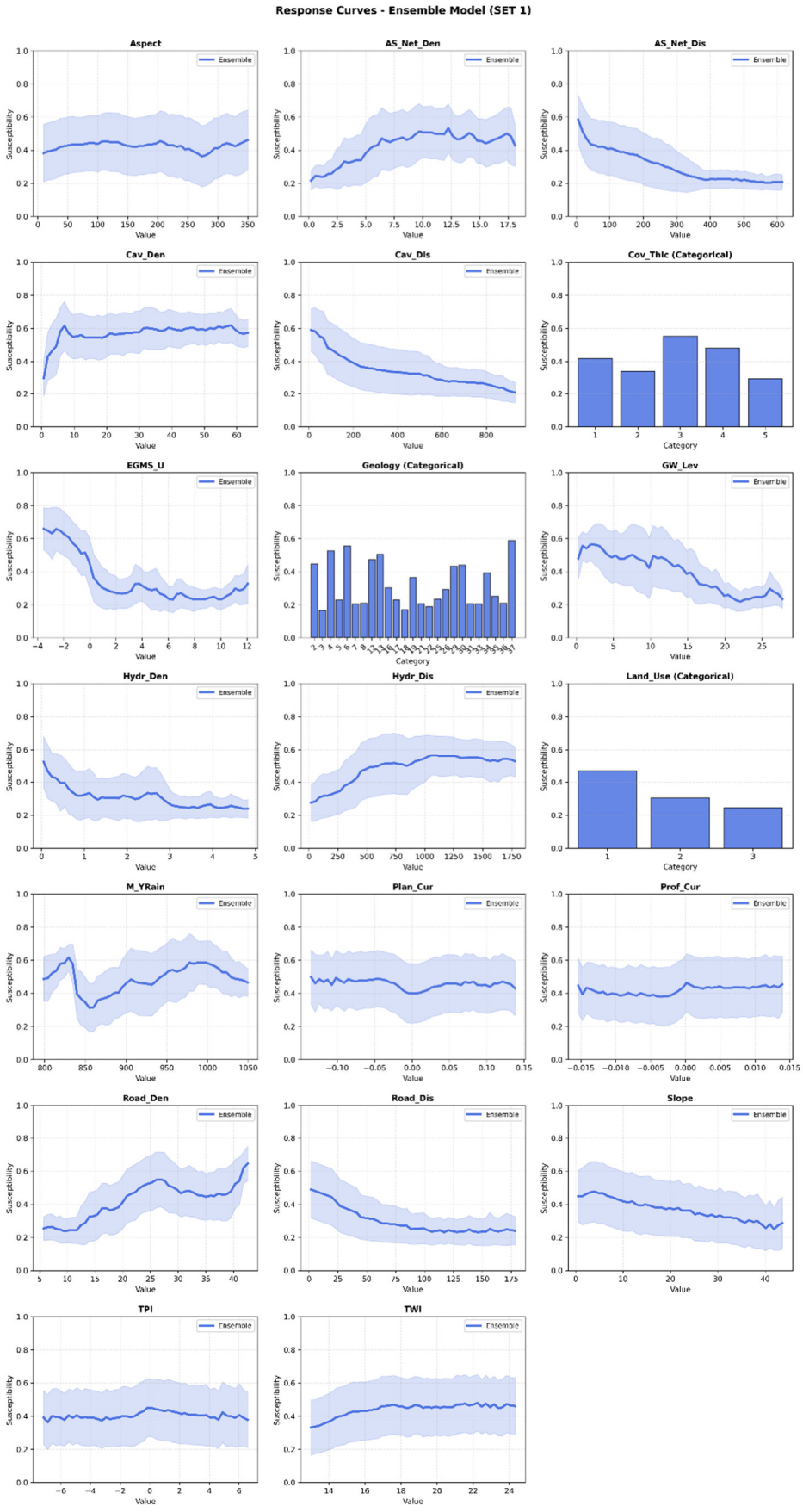

Figure 8 - Response curves for Group 1.

The performance obtained are acceptable, in particular, the performance score for the Group 1 susceptibility map are ROC/AUC = 0.90 (Fig. 9a), sTSS = 0.875, Specificity = 0.917, and Sensitivity = 0.833. Regarding Group 2, the scores are ROC/AUC = 0.83 (Fig. 9b), sTSS = 0.816, Specificity = 0.632, and Sensitivity = 1.000, while the remaining Group 3 scores are ROC/AUC = 0.87 (Fig. 9c), sTSS = 0.806, Specificity = 0.778, and Sensitivity = 0.833.

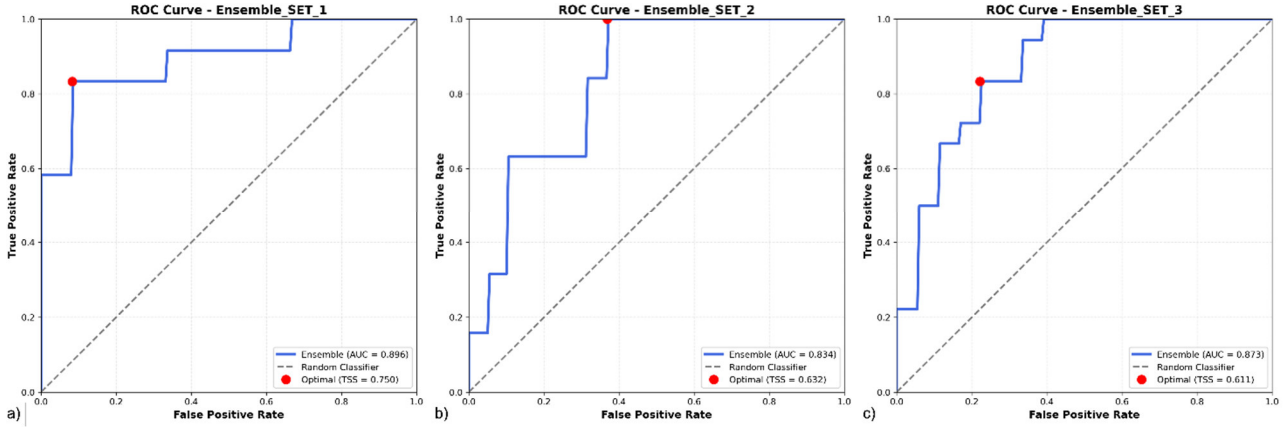

Figure 9 - ROC/AUC diagram for a) Group 1, b) Group 2, and 3) Group 3.

Sinkholes – GI scenarios

The sinkhole susceptibility map obtained showcase the influence of the predisposing factors on the final product. The anthropogenic sinkhole susceptibility for the Group 1 (Fig. 10) is the one with the most severe susceptibility, showing the influence of both the distance to networks layers and the density ones.

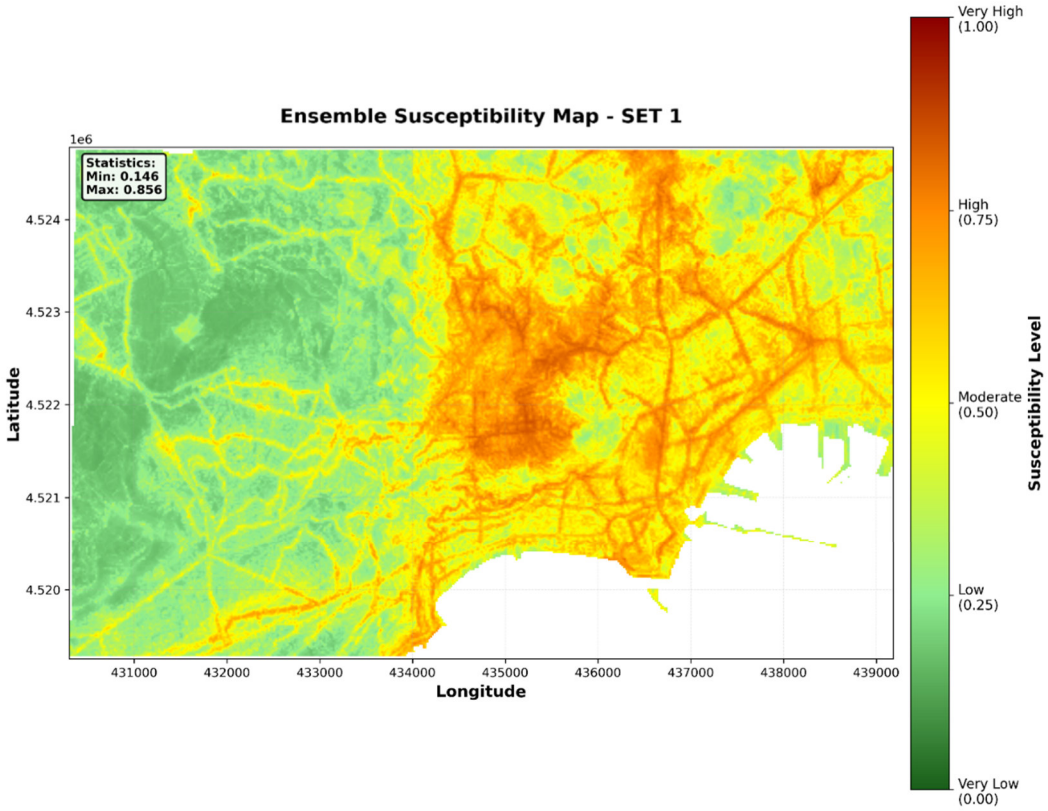

Figure 10 - Anthropogenic Sinkhole Susceptibility map for Group 1.

On the other hand, the anthropogenic sinkhole susceptibility map for the Group 2 dataset showcases less severe condition and it is highly influenced by the distance to the network rasters, especially road and main aqueduct and sewers, as shown in Fig. 11.

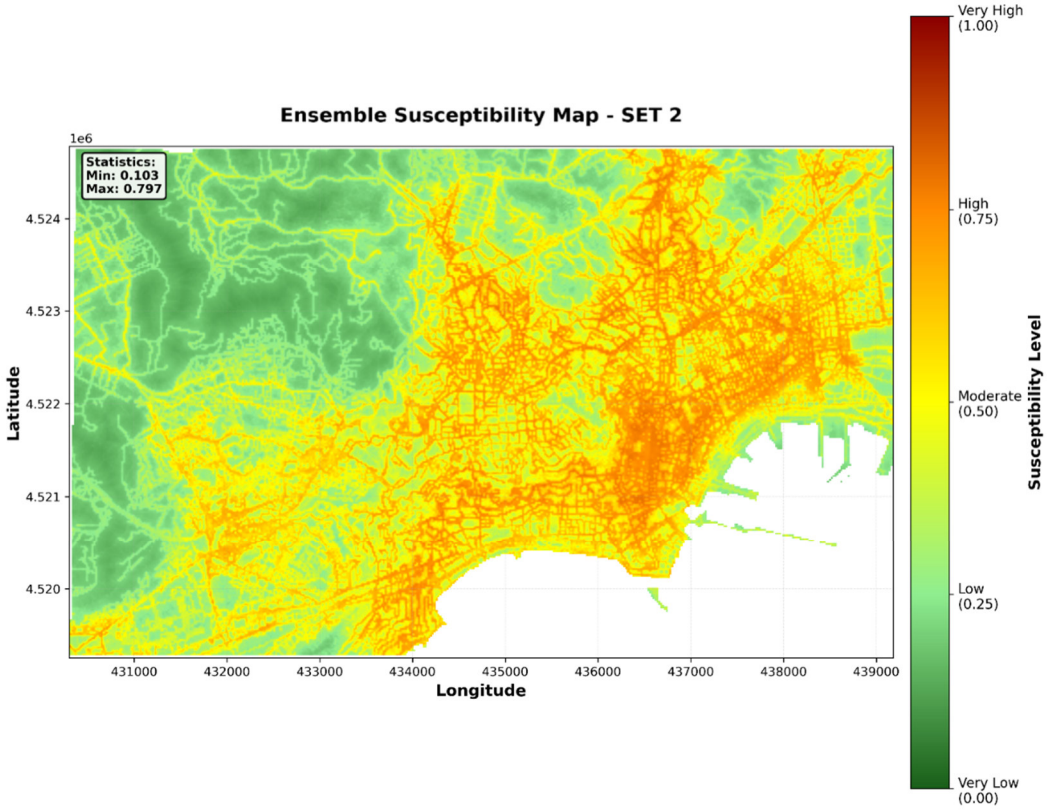

Figure 11 - Anthropogenic Sinkhole Susceptibility map for Group 2.

The sinkhole susceptibility map for Group 3 (Fig. 12) shares some similarities with the Group 1 susceptibility map, although the susceptibility seems to be less severe with slightly lower occurrence probability.

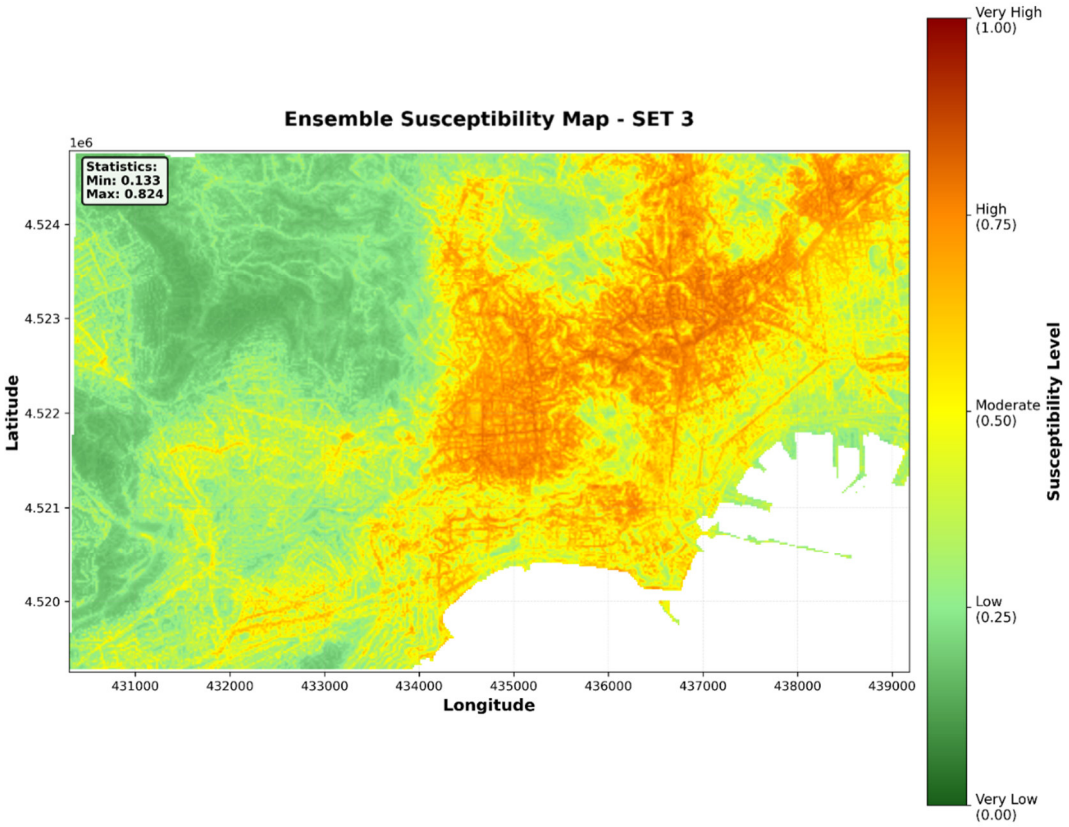

Figure 12 - Anthropogenic Sinkhole Susceptibility map for Group 3.

All three susceptibility maps are characterized by Very Low areas related to the hillslopes of the Camaldoli Hill (top-left corner of the maps) and the slopes surrounding the Agnano plain (left side of the maps). Meanwhile, the most affected areas of the maps are the ones related to high-density residential areas (City Center and top of the Vomero Hill). After dividing the susceptibility map into 5 different classes using the Natural Breaks method, the analysis of the areal extension for every class highlights a decreasing trend from Very Low to Very High susceptibility.

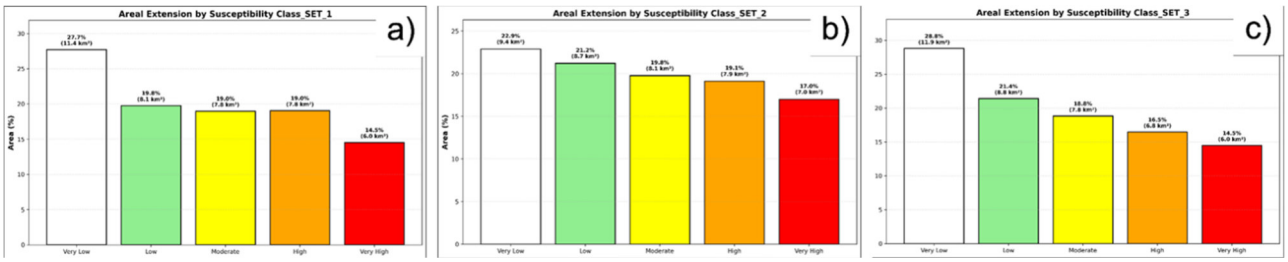

Figure 13 - Percentage of area attributed to each susceptibility class for Group a) 1, b) 2, and c) 3.

Debris flow – Predisposition

For the debris-flow component of the City of Naples Demonstration Case, slope predisposition was assessed by applying the Parsifal_T_dry module to the volcanic slopes of Camaldoli Hill. In this Demonstration Case, and for the purposes of illustrating the applicability of the toolchain, a conservative stability threshold of FoS = 1.3 was adopted instead of the classical FoS = 1.0. This allows identifying not only conditions of actual failure, but also sectors characterised by a reduced stability margin.

Morphological attributes and cover-thickness distributions were derived from a high-resolution DTM and from the available reconstruction of the volcaniclastic mantle, which together define the geometrical and stratigraphic setting of the soil cover (Fig. 14). Geotechnical parameters were assigned to the volcaniclastic deposits based on literature and available tests, adopting representative values of effective cohesion ($c = 6$ kPa), friction angle ($\varphi = 33°$) and unit weight ($\gamma n = 13.65$ kN/m³). These inputs were used to compute the Factor of Safety under dry and static conditions, providing a first-order picture of the spatial variability of slope stability across the Camaldoli area.

It is important to note that the resulting FoS map in Fig. 15 does not highlight areas with FoS < 1.3, but rather illustrates the spatial contrast in static stability prior to the application of hydrological or seismic triggering. Steeper slopes and channel-head areas, where cover thickness and inclination combine unfavourably, are associated with lower FoS values, indicating a higher predisposition to shallow sliding and potential debris-flow initiation. Gentler slopes and convex interfluves are instead characterised by FoS values generally above unity, suggesting a lower likelihood of failure in dry conditions. This "static" predisposition layer represents the baseline upon which hydrological and seismic perturbations are subsequently imposed.

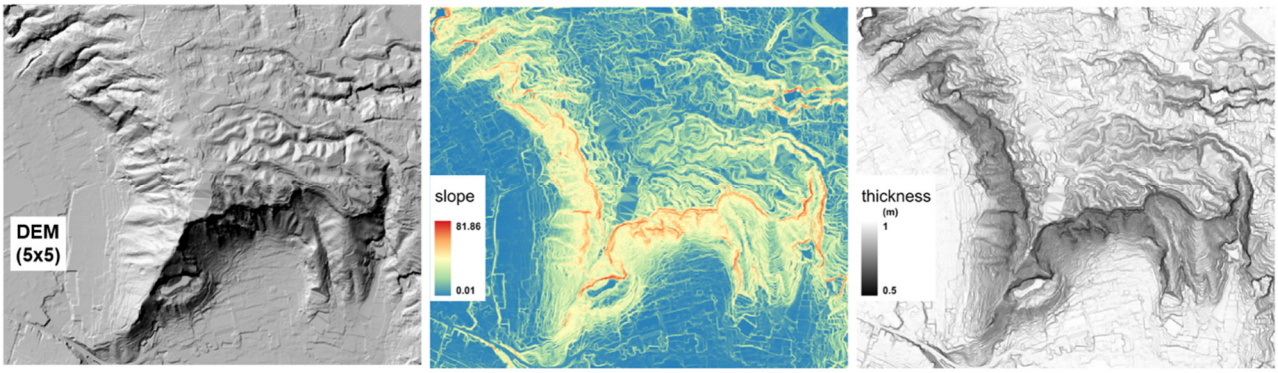

Figure 14 – Morphological and cover thickness input rasters for Parsifal_T_dry application.

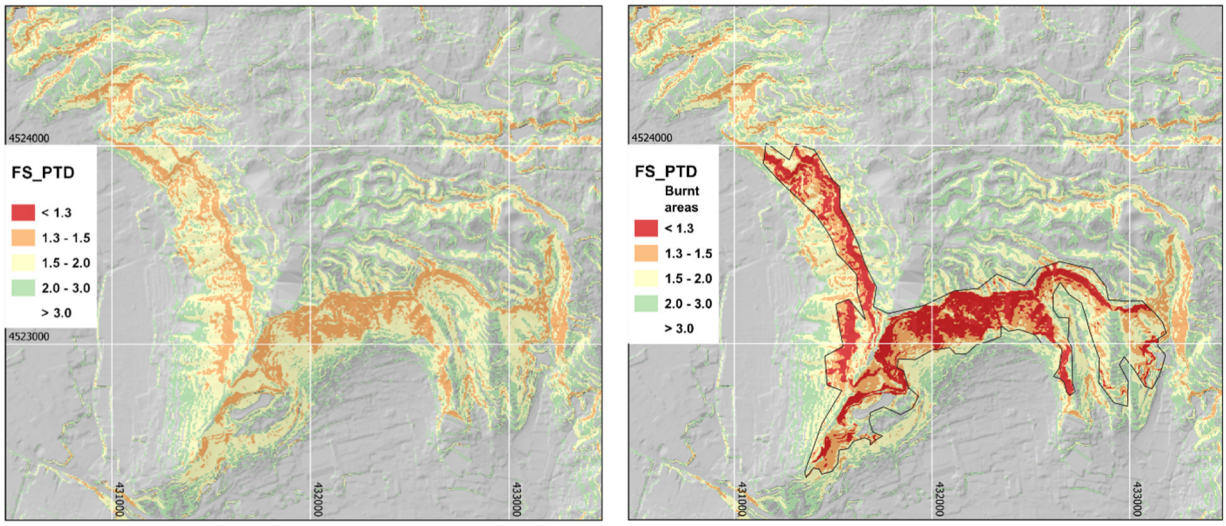

Figure 15 - Factor of Safety maps under dry and static conditions (left) and considering the presence of burnt areas (right). Burnt areas are outlined in black.

Debris flow – Preparation and triggering

The first analysis of the preparation factors encompassed wildfires, in terms of reduction in cohesion for the burnt areas, considering an event that occurred in Camaldoli Hill in June 2024. Specifically, for demonstration purposes, a reduction in cohesion from 6 to 4 kPa was assumed, according to Schmidt et al. (2001) and Evangelista & Scotto di Santolo, (2004). Figure 15 shows the effect on the FoS, calculated under dry conditions (FS_PTD), with a significant increase in the area characterized by values lower than 1.3. In particular, the map on the right highlights a marked expansion of low-stability zones (FS < 1.3) within the burned areas, indicating a substantial reduction in slope stability due to the decrease in soil cohesion following the wildfire.

Moreover, the preparation and triggering stages for debris-flow susceptibility were analysed by exploring a set of hydrological and seismic scenarios using the Parsifal_T_wet and Parsifal_T_s modules. Rather than explicitly modelling the full rainfall–runoff process, the hydrological forcing was represented through RU scenarios, where RU is defined as the ratio between saturated and total soil thickness. Two synthetic saturation conditions were considered, RU = 0.2 and RU = 0.5, reflecting moderately wet and highly saturated states of the volcaniclastic cover. These RU values were imposed on the previously derived geomorphological and geotechnical configuration to obtain FoS maps under increasing degrees of saturation.

Seismic triggering was analysed by coupling each hydrological state with a corresponding seismic scenario via Parsifal_T_s. For each configuration, a maximum expected acceleration (ACmax) was assigned and used to compute seismically induced reductions in FoS. The combination of hydrological and seismic conditions explored is summarised in Table 5, which reports the suite of simulations performed: a purely dry–static case (FS_PTD), a dry–seismic case (FS_PTDS), two wet scenarios at RU = 0.2 with and without seismic loading (FS_PTW2, FS_PTW2S), and two wet scenarios at RU = 0.5, again with and without seismic forcing (FS_PTW5, FS_PTW5S).

The spatial patterns of the resulting FoS maps (Fig. 16) show a progressive reduction in stability as RU increases, with a marked expansion of areas characterised by FoS values approaching or falling below the adopted threshold of 1.3. The introduction of seismic loading further decreases FoS in already fragile sectors, particularly along steep slopes and channel heads, where the combined effects of saturation and ground shaking produce the most critical conditions. This set of simulations provides a consistent

framework for identifying those parts of the Camaldoli slopes that are most prone to failure under different hydrological and seismic scenarios and forms the basis for subsequent GI scenario construction.

Table 5 - Summary of the Parsifal simulation in the Camaldoli hill.

Hydrologic condition	dry	dry	wet RU=0.2	wet RU=0.2	wet RU=0.5	wet RU=0.5
Seismic condition	static	seismic AC_{max}=0.69g	static	seismic AC_{max}=0.66g	static	seismic AC_{max}=0.51g
Output name	FS_PTD	FS_PTDS	FS_PTW2	FS_PTW2S	FS_PTW5	FS_PTW5S

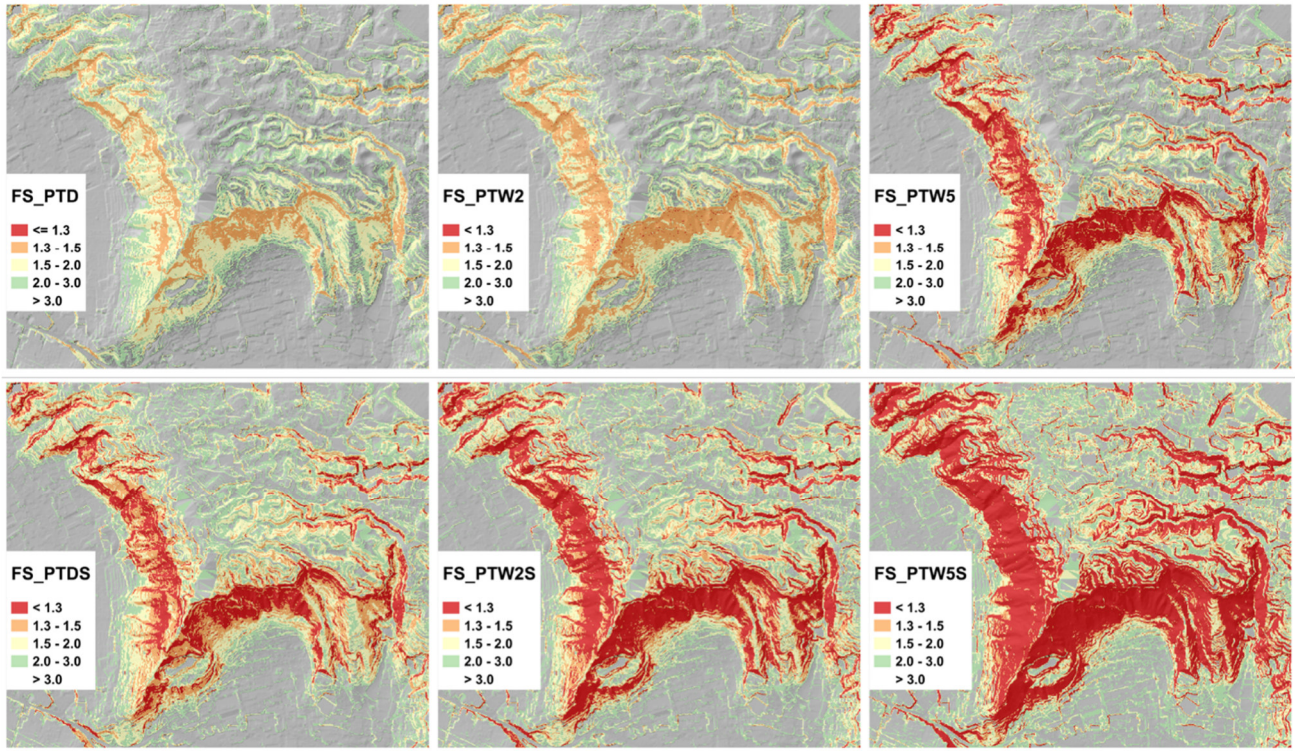

Figure 16 - Factor of Safety maps under different simulation conditions (see Tab.5) for the Camaldoli hill.

Debris flow – GI scenarios

GI scenarios for debris flows were derived by combining the FoS results obtained with Parsifal with a morphological estimation of potentially mobilisable volumes. For each simulation, areas with FoS < 1.3 were delineated and intersected with a slope-unit partition of the study area. Within each unstable slope unit, a simplified morphometric procedure was applied to approximate the thickness of material potentially involved in failure, allowing for an order-of-magnitude estimation of debris volumes that could be mobilised under the considered triggering conditions. The spatial distribution of these estimated volumes is shown in Fig. 17, which emphasises the concentration of larger potential source volumes along the steepest portions of the Camaldoli slopes and in proximity to channel heads.

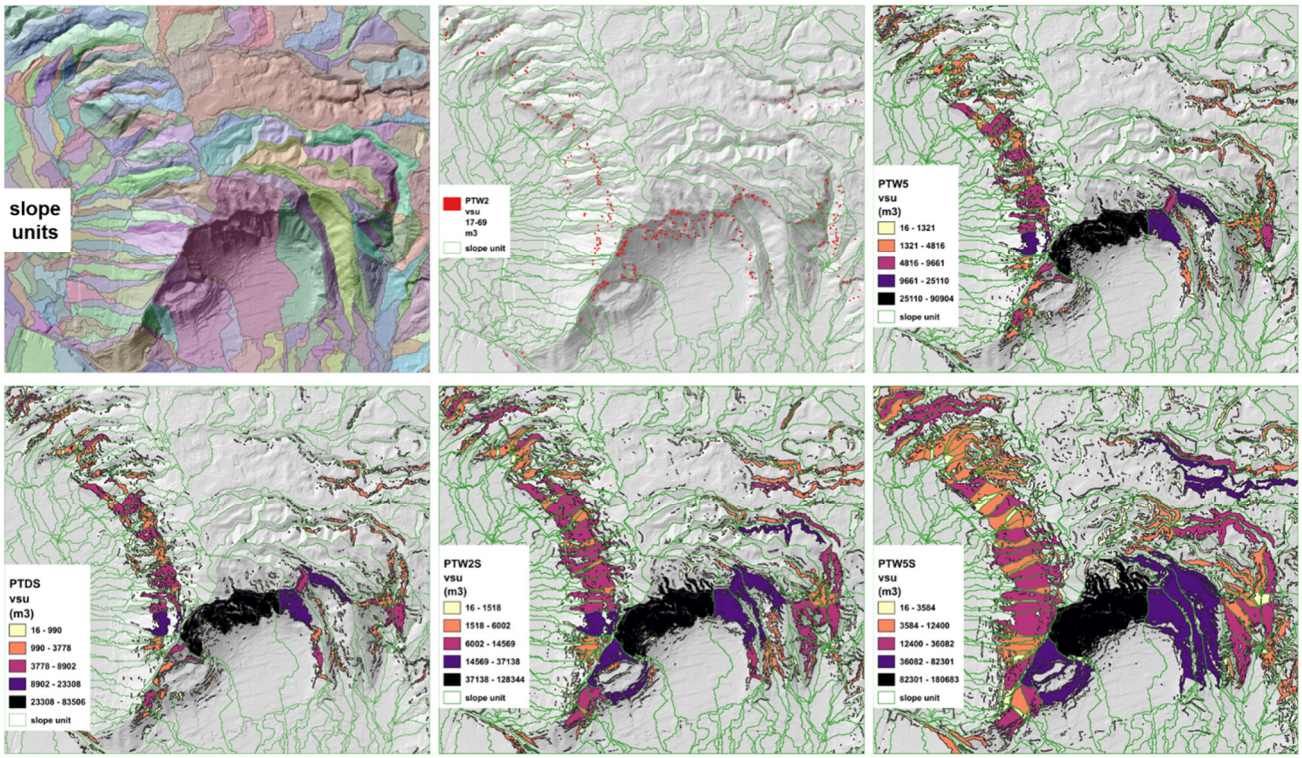

Figure 17 - Volume estimation within the slope units.

6.2. Landslides of Calabria demonstration case

Rockfall – Predisposition

The application of the STONE model in Calabria demonstration case allowed a detailed reconstruction of the potential behaviour of falling blocks along the coastal sector between Paola and Fuscaldo. The high-resolution LiDAR DTM (2 m) enabled an accurate representation of the steep slopes, rocky scarps, gullies and slope breaks that control the propagation mechanisms. The potential source areas, derived through the multi-threshold morphometric approach, are continuously distributed along the rocky walls that border the coastal ridges (Fig. 18). They coincide with scarps predisposed by the geological setting , i.e. composed of competent and fractured rock masses, are associated with high slope values and positive curvature, and delineate morphological niches predisposed to block detachment. Their spatial continuity indicates that rockfall initiation may involve wide portions of the slope rather than isolated unstable points.

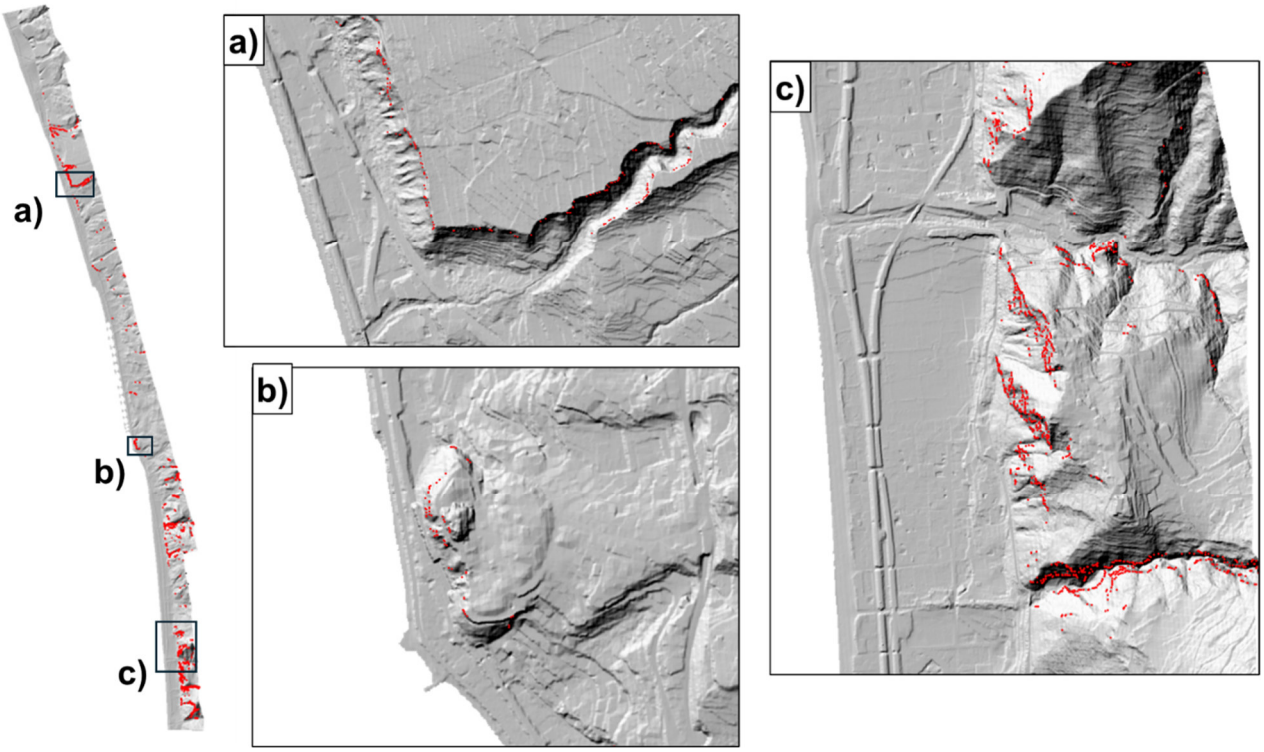

Figure 18 – Rockfall source areas identified through the morphometric multiple-threshold procedure.

Rockfall – GI scenarios

The STONE simulations performed for the Calabria DC provide a detailed reconstruction of potential rockfall trajectories originating from the morphometrically derived source areas. The results reflect the strong morphological control exerted by the steep crystalline slopes that dominate the coastal escarpment, where source cells are aligned along high-angle ridges, niche-like features and gully heads. The resulting propagation patterns show clear spatial partitioning into three geomorphological sectors—northern, central and southern—which display distinct runout behaviors in accordance with local topographic constraints (Figs. 19–20).

In the northern sector, the simulated trajectories are generally short and confined to the upper portion of the slope. Blocks detach from steep scarps but rapidly decelerate on the downslope surfaces, where slope gradients decrease and terrain roughness increases. The trajectories tend to disperse laterally and do not exhibit strong channelization, reflecting the broader, less incised morphology that characterizes this part of the escarpment. As visible in the corresponding map, trajectories dissipate well upslope from the coastal corridor and remain distant from the railway alignment, with no direct or potential interaction with the infrastructure.

A raster-based inspection confirms that the few isolated activated cells occurring near the railway line in this sector correspond to marginal raster artefacts rather than coherent runout paths. Therefore, the northern sector does not present conditions predisposing to rockfall propagation toward the railway.

The central sector exhibits the most critical configuration and represents the portion of the slope where rockfall processes may pose a potential exposure to the railway infrastructure. Here, detachment areas coincide with very steep rock walls and incised gullies that act as preferential channels for block propagation. The resulting trajectories are longer, more concentrated and display strong channelling effects, producing high-density runout patterns that extend farther downslope than in the other sectors.

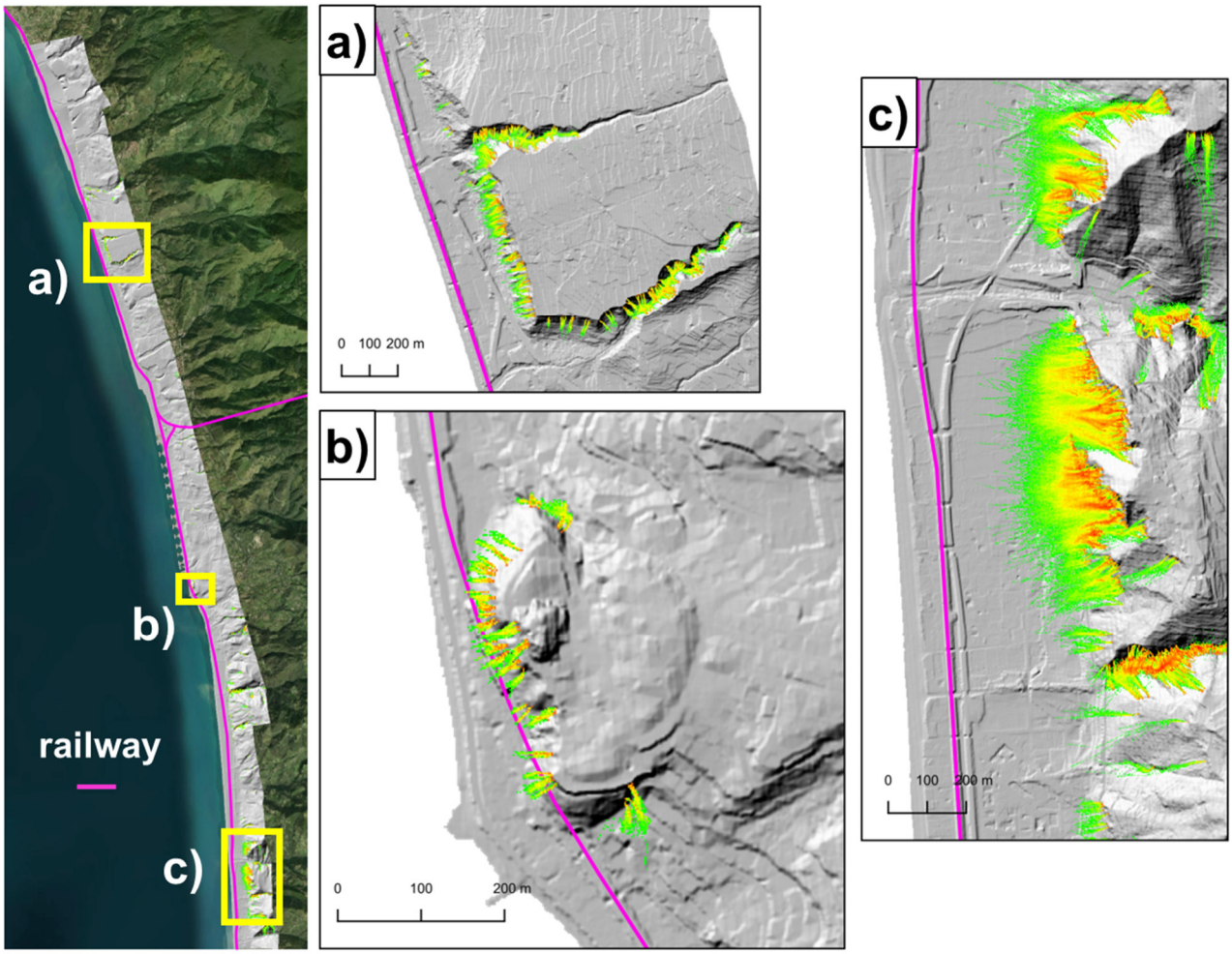

Figure 19 - Results of the STONE simulations, with detail on the three morphologically distinct sectors: a) northern sector, b) central sector, c) southern sector.

In the detailed view of this area (Fig. 20), a subset of trajectories is seen to potentially intersect or reach the railway alignment, both at the entrance of a tunnel and along a short uncovered track segment. This behaviour is consistent with the local morphology: the railway lies at the base of a narrow gully where runout energy is only partially dissipated, and the absence of wide depositional benches allows blocks to maintain sufficient momentum downslope. The raster analysis corroborates this interpretation: while isolated activated pixels near the railway occur in all sectors, only in the central sector do these correspond to the envelope of coherent STONE trajectories, confirming the higher susceptibility of this area to rockfall–infrastructure interaction under unfavourable detachment conditions.

The southern sector is characterized by more continuous slopes and less pronounced channel confinement than the central one. Simulated trajectories are moderately long but tend to disperse over a broader downslope area, leading to partial energy dissipation before reaching the coastal plateau. Despite the higher slope continuity, trajectories do not approach the railway line, and no potentially interacting runout paths are observed in the map. As in the northern sector, any raster cells located near the railway are attributable to marginal discretization artefacts rather than to physically meaningful trajectories. Overall, the southern sector does not show runout conditions that would lead to a potential impact on the railway under the simulated scenarios.

The integrated analysis of the three sectors indicates that the central sector is the only portion of the slope where STONE simulations produce trajectories that may potentially intersect or reach the railway alignment, particularly at a tunnel entrance and over a short open-air stretch. In contrast, the northern and southern sectors show no evidence of exposure, with trajectory envelopes remaining entirely upslope. This spatial differentiation is crucial for defining priority areas for mitigation and for supporting subsequent steps of the RETURN project related to risk analysis and scenario evaluation.

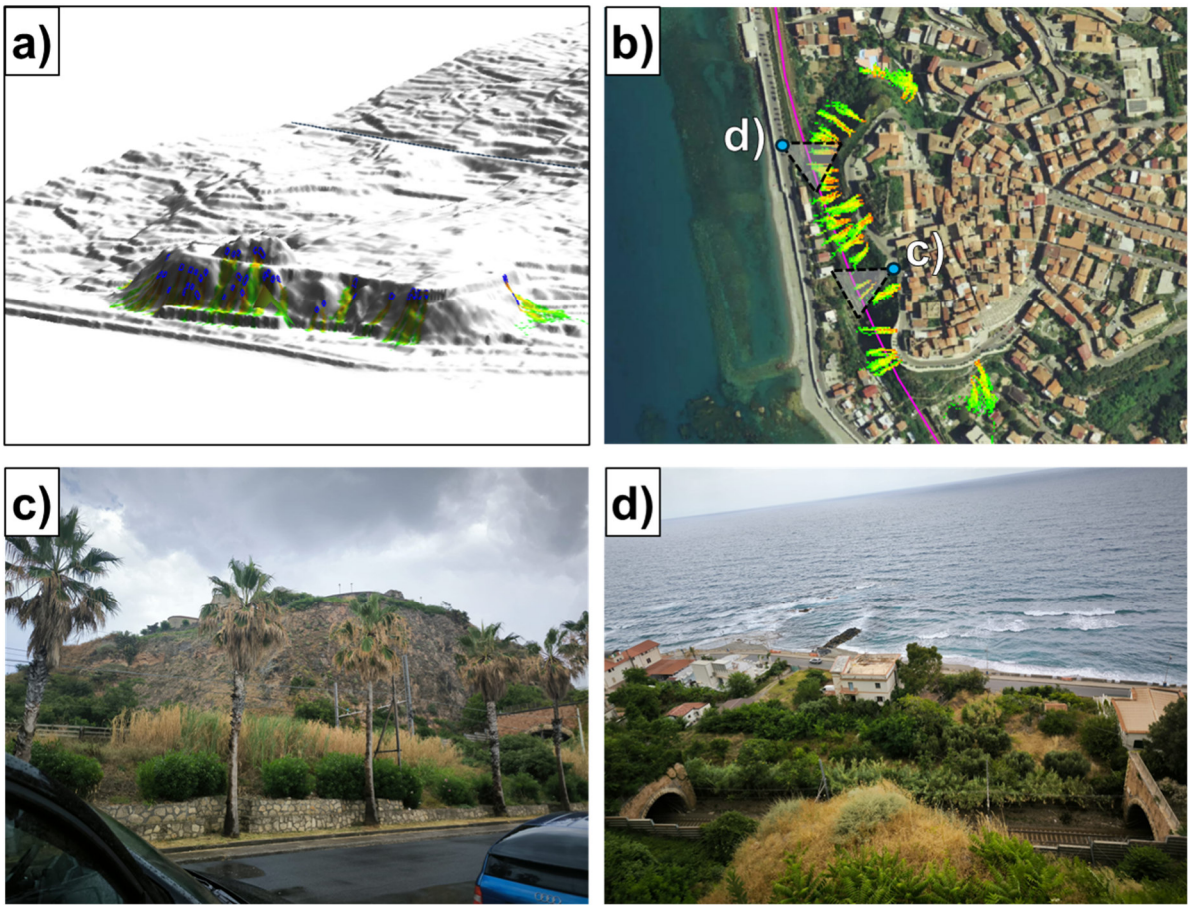

Figure 20 - Detail of the central sector showing the proximity between STONE-simulated trajectories and the railway alignment. a–c) Maps of the potentially interacting trajectories. d) Photographs taken during field surveys conducted in July 2024.

Debris flow – Predisposition

The predisposition analysis for the Fuscaldo sector of the Calabria DC focused on the terminal portion of the Maddalena catchment in Fuscaldo area (CS), a steep crystalline basin draining directly toward the coastal plain. The evaluation of static stability was performed using Parsifal_T_dry, adopting two initial degrees of soil saturation—RU = 0.3 and RU = 0.5—representing, respectively, minimum and intermediate antecedent wetness conditions. These values were chosen based on the typical hydrological behaviour of the thin weathered mantles that develop over metamorphic bedrock in this area.

Morphological and cover-thickness parameters were derived from the high-resolution DTM and from the reconstructed soil-depth model (Fig. 21), which together define the geometry and mechanical stratigraphy of the debris-mantled slopes. Geotechnical parameters assigned to the volcaniclastic and colluvial soils fall within ranges documented for the area: effective cohesion c = 2–8 kPa, friction angle φ = 23–33°, and unit weight γ_n = 17–18 kN/m³, capturing the spatial variability of soil mechanical properties observed in field conditions.

The resulting static Factor of Safety maps (Fig. 22) show no significant difference between the FoS distributions calculated for the two initial saturation values (RU = 0.3 and RU = 0.5). This reflects the fact that, under dry conditions, the mechanical response of the slope is dominated by steep topography and limited soil thickness, rather than by variations in antecedent saturation. These FoS maps constitute the baseline for subsequent triggering analyses.

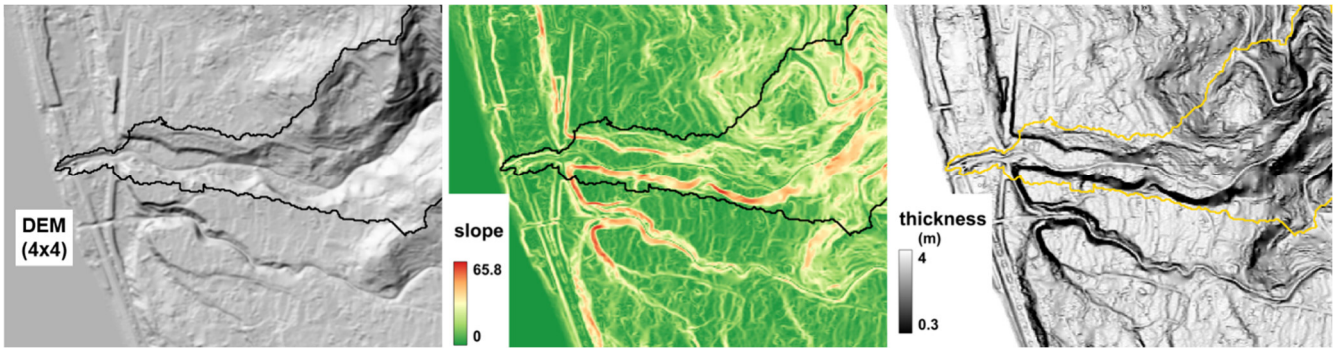

Figure 21 - Morphological and cover thickness input rasters for Parsifal_T_dry application.

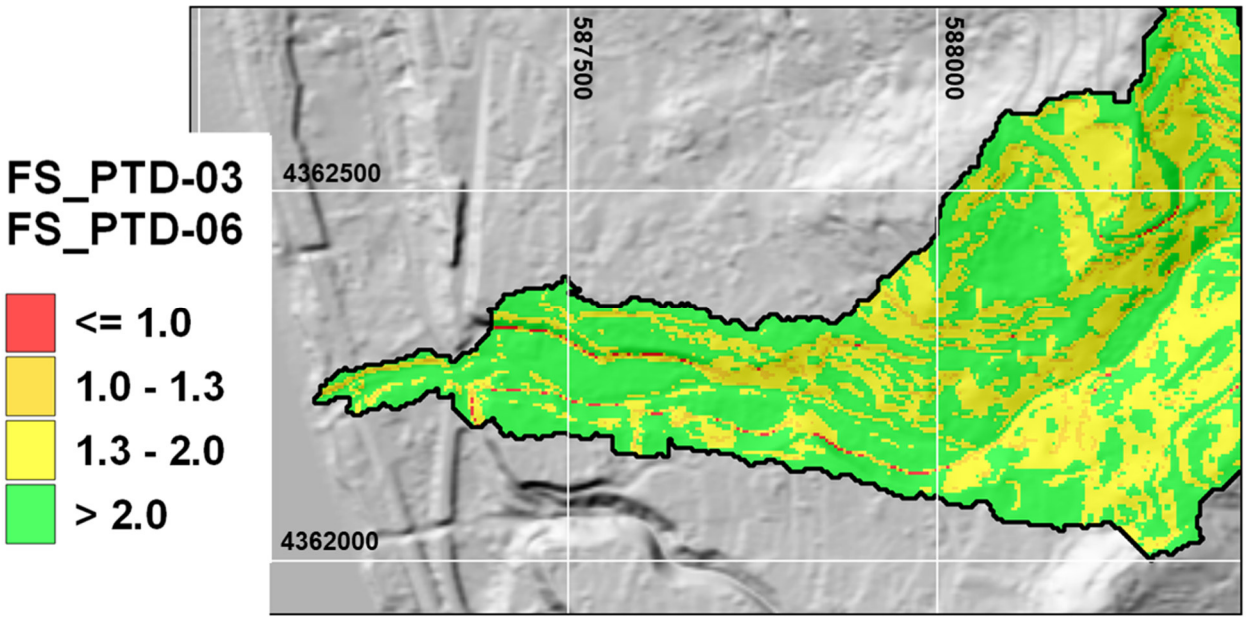

Figure 22 - Factor of Safety map for dry and static conditions and both the initial RU (0.3 and 0.6).

Debris flow – Preparation and triggering

Triggering conditions were explored using Parsifal_T_wet and Parsifal_T_s, combining hydrological forcing derived from TOPMODEL with seismic loading. As shown in Table 6, eight simulation scenarios were performed by systematically combining:

- two initial RU values: 0.3 and 0.6
- two hydrological conditions: dry vs. wet* (the latter obtained from TOPMODEL using a rainfall intensity of 65 mm/h, based on FOCA dataset; Claps et al., 2024)
- two seismic conditions: static vs. seismic

Wet conditions derived from TOPMODEL represent an explicit hydrological response to the FOCA rainfall scenario, resulting in increased saturation levels that reduce slope stability and modify the spatial pattern of pore-pressure build-up.

The resulting FoS maps (Fig. 23) show a progressive reduction in stability as hydrological and seismic forcing increases. Hydrological loading alone (FS_PTW-03 and FS_PTW-06) produces a marked decrease in FoS across the slope units located in the upper and middle portions of the basin, with the most significant instabilities emerging along channel heads and concave slopes where soil thickness is locally greater. When seismic loading is added (FS_PTWS-03 and FS_PTWS-06), these unstable patches expand and coalesce, indicating a more pervasive response of the slope system to combined forcing.

A complementary representation of slope fragility is provided by the critical acceleration maps (Fig. 24), which quantify the additional ground shaking needed to induce failure under each hydrological state. As expected, critical acceleration decreases for wet conditions, particularly where saturation derived from TOPMODEL

is highest. These patterns are consistent with the geomorphological configuration of the Maddalena basin and highlight the sectors most sensitive to hydrological–seismic interactions.

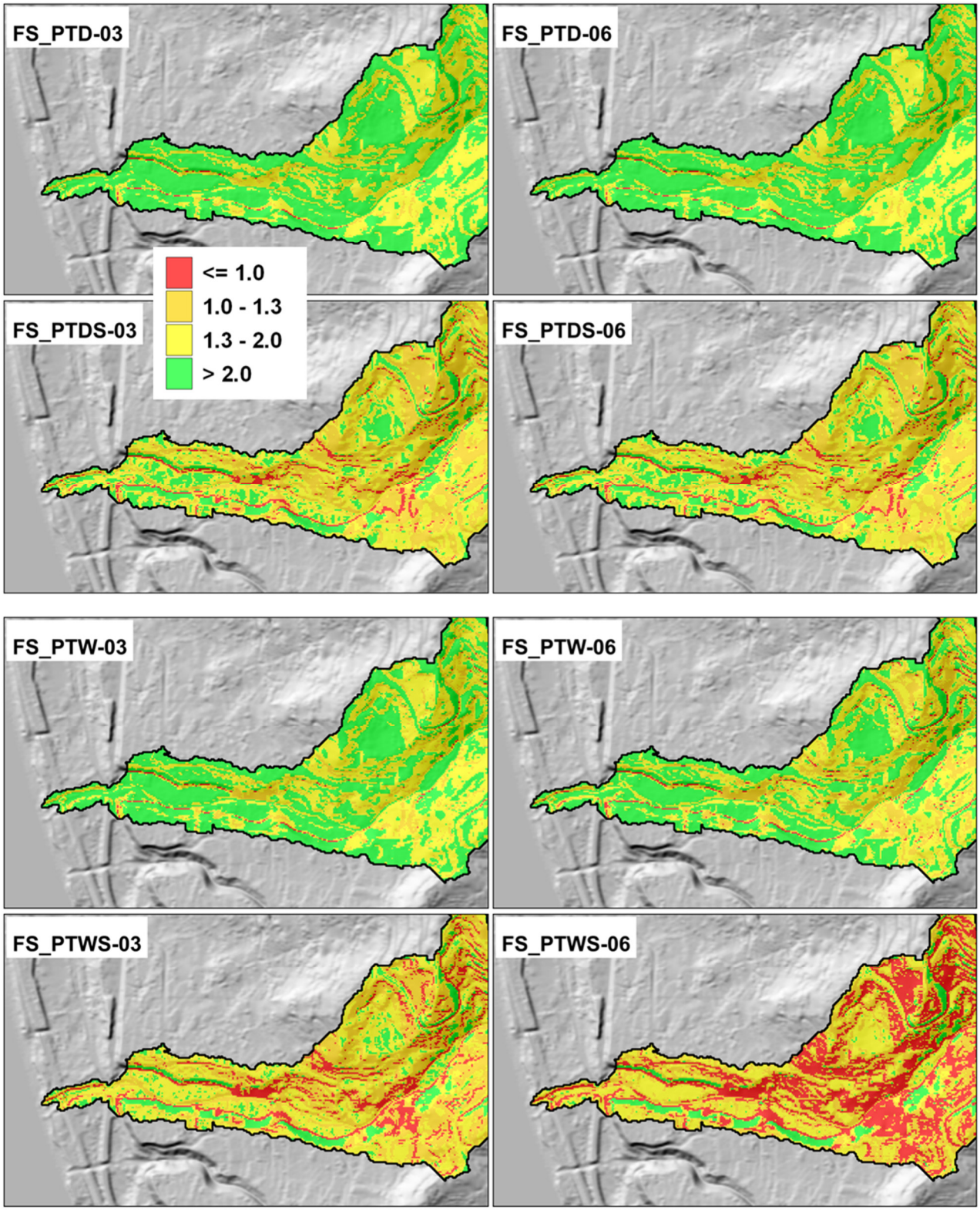

Figure 23 – Factor of Safety maps under different simulation conditions (see Tab.6) for the Fuscaldo area.

Table 6 - Summary of the Parsifal simulation in the Fuscaldo area. *wet condition derived from TOPMODEL. Underlined output names are used for GI scenarios analysis. **simulation considered for runout analysis with RASH3D.

Initial RU	0.3	0.6	0.3	0.6	0.3	0.6	0.3	0.6
Hydrologic condition	dry		dry		wet*		wet*	
Seismic condition	static		seismic		static		seismic	
Output name	FS_PTD-03	FS_PTD-06	FS_PTDS-03	FS_PTDS-06	FS_PTW-03 **	FS_PTW-06	FS_PTWS-03	FS_PTWS-06

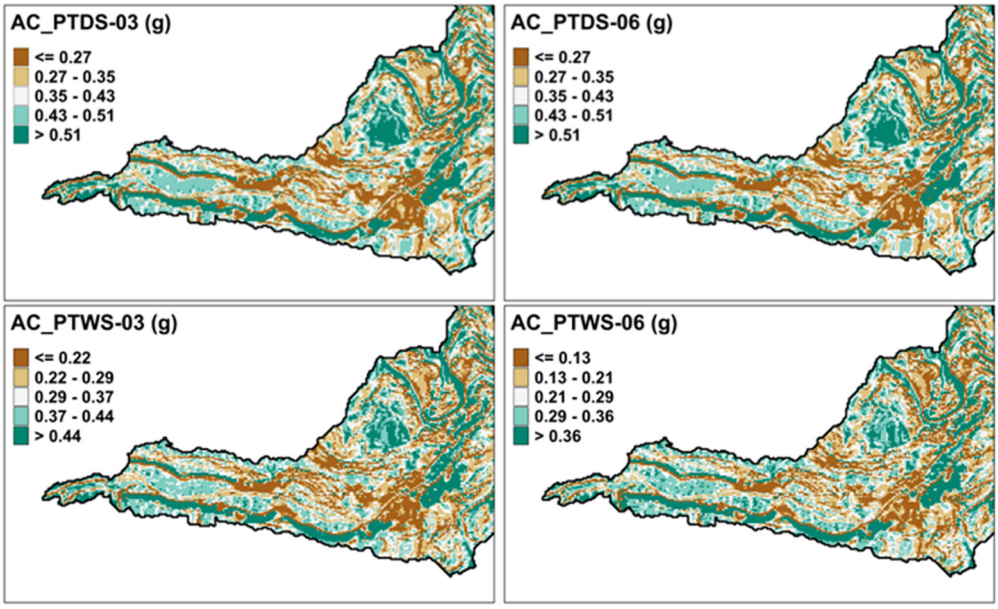

Figure 24 - Critical acceleration calculated for different hydrological conditions.

Debris flow – GI scenarios

GI scenarios were constructed using the Parsifal outputs identified in Table 6 (underlined cases), focusing on those where hydrological and seismic perturbations drive FoS values below unity. Prior to scenario derivation, a filtering procedure was applied to remove anomalous unstable pixels that were inconsistent with local morphology; this step was guided by expert judgment, ensuring that only physically plausible instability zones were retained.

The resulting maps of FoS < 1 were intersected with slope units to delineate potential initiation areas for shallow failures. Within these unstable slope units, a morphological volume estimation procedure was applied to quantify the amount of material potentially mobilisable under each scenario. The spatial distribution of these volumes (Fig. 25) shows that the largest potentially mobilisable masses are located along the main headwater hollows and the transitional slope segments feeding the debris-flow channel.

These potential source volumes represent the basis for the subsequent runout modelling with RASH3D, which is applied to a selected sector of the Maddalena basin (Fig. 25) to reconstruct the possible downstream propagation of debris flows. In the reported simulation (Fig. 26), the scenario FS_PTW-03 has been considered. From this scenario, the area characterized by a higher concentration of unstable cells and realistic slope values with respect to the triggering of debris-flow phenomena was selected and analyzed. This area is particularly significant, as historical imagery clearly indicates that it was affected by wildfires in the recent past. However, the effects of wildfire were not considered in the triggering analysis.

The runout was simulated using the Voellmy rheology, which has been successfully applied to debris flows by several authors (e.g., Rickenmann and Koch, 1977). The basal friction coefficient used in the simulation is 0.2, while the turbulence coefficient is 500 m/s². These parameters were selected based on the authors' experience and on values reported in the literature. Figure 26 shows the runout path together with the deposited mass.

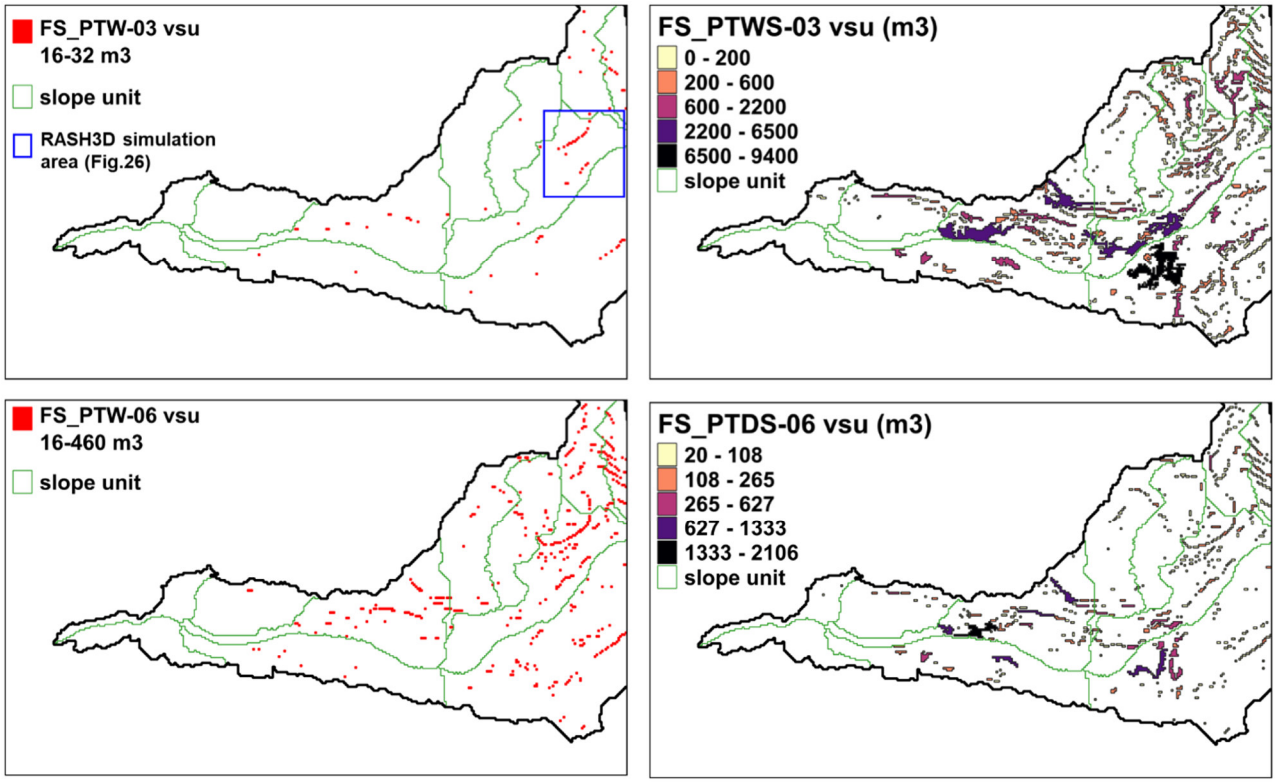

Figure 25 - Volume estimation within the slope units for the selected output.

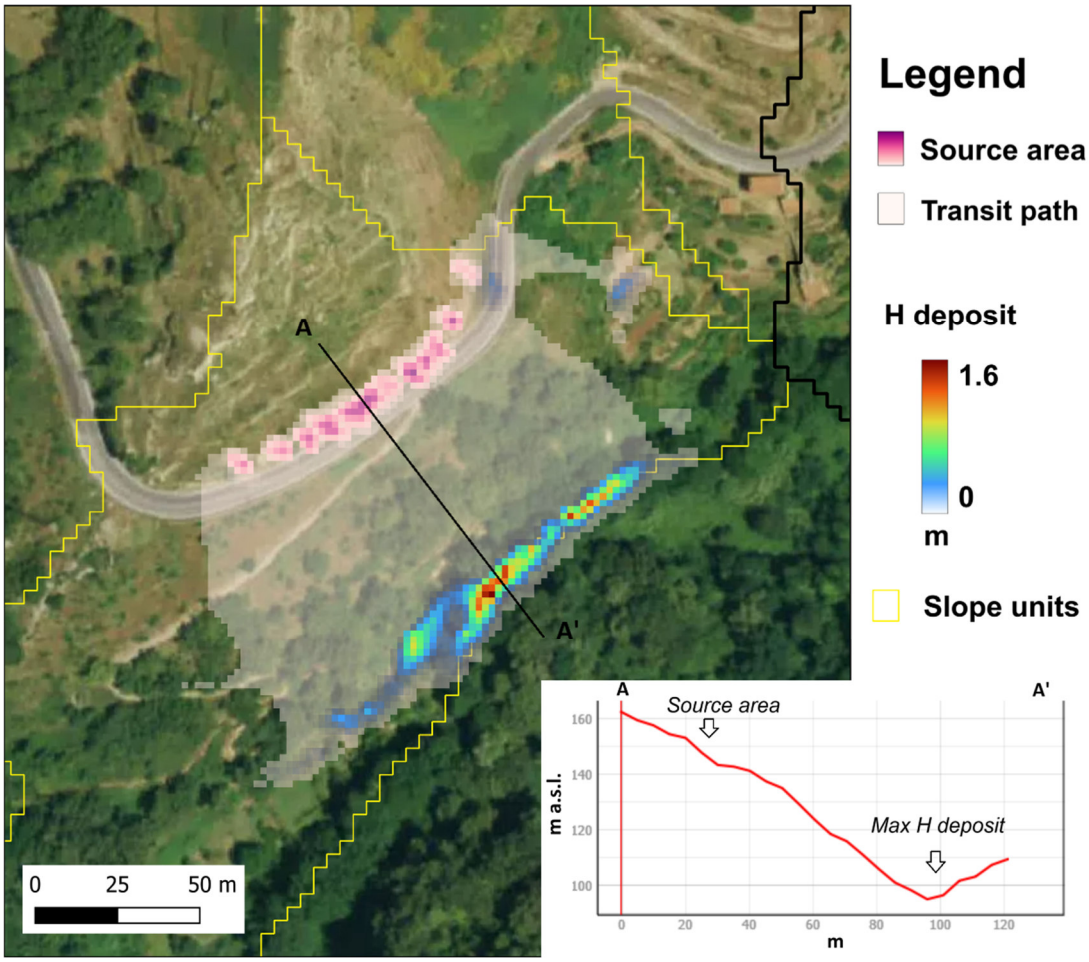

Figure 26 - Results of RASH3D for the simulation FS_PTW-03.

6.3. Debris flows of the Alemagna DC

Predisposition

The susceptibility analysis was carried out using the WP2 Box tool. Weight of Evidence (WoE; Van Westen, 1993) method was adopted to perform susceptibility analysis. This method quantifies the strength of association between predictor variables and the occurrence of a binary outcome, such as landslide occurrence. It calculates the weight of evidence for each predictor variable, indicating its influence on the outcome variable. WoE assesses the odds of the event occurring in the presence of a particular predictor variable compared to its absence.

Debris flow landslides PIFFs (Punto Identificativo Fenomeno Franoso – Landslide Phenomenon Identifier Point) were considered as presence points. A total of 270 presence points were selected.

A total of 9 predictor variables were employed with a resolution of 10 meters × 10 meters, i.e.:

- Aspect;
- Channel Network Distance;
- Lithology;
- Land_Use;
- Planar Curvature;
- Profile Curvature;
- Relative Slope Position;
- Slope;
- Topographic Wetness Index.

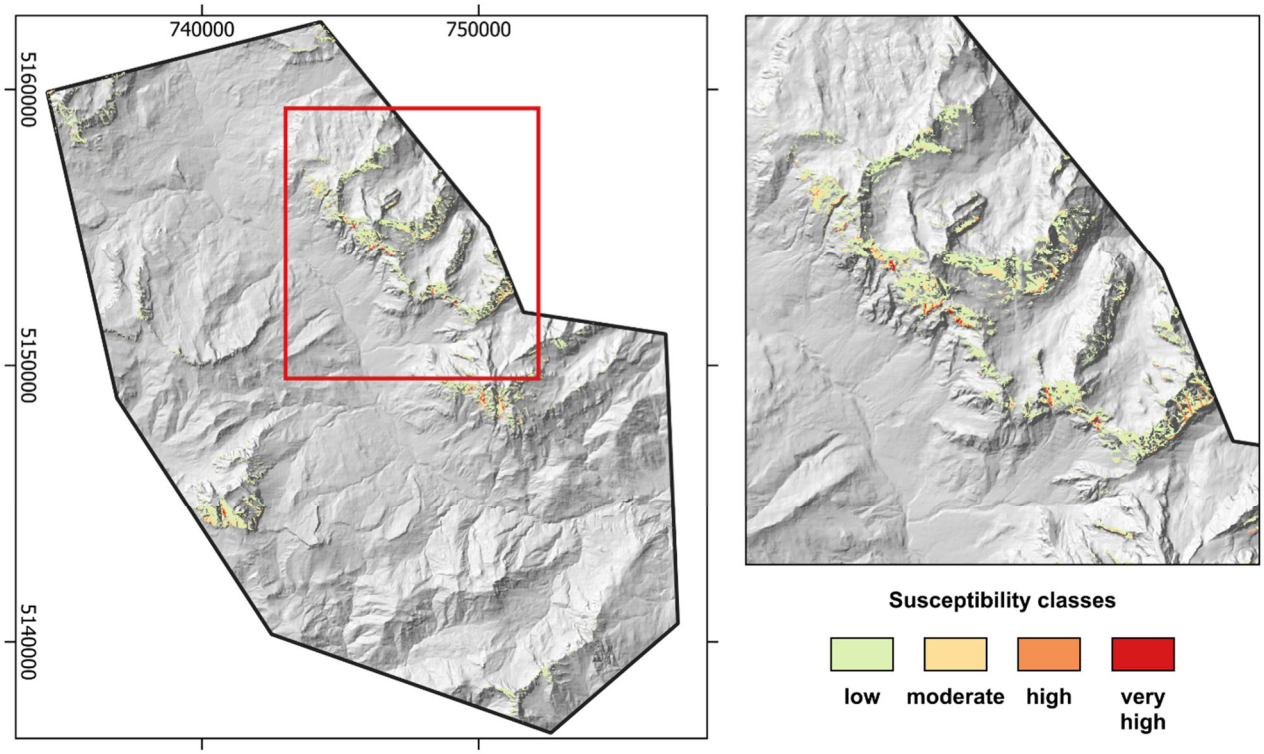

Figure 27 - Susceptibility map of Alemagna DC.

Figure 27 shows the spatial distribution of the susceptibility classes obtained from the WoE analysis. Areas characterised by higher susceptibility are mainly located along steep lateral slopes and in correspondence with small headwater catchments draining towards the Boite Valley. These sectors typically coincide with high slope gradients, short distances from the channel network and geomorphological settings favourable to sediment accumulation and mobilisation.

A clear concentration of medium to high susceptibility values can be observed along tributary basins connected to the main drainage network. These channels represent preferential pathways for debris-flow initiation and propagation, reflecting the strong control exerted by topography and hydrological connectivity on the spatial distribution of the process. Conversely, the valley floor and gently sloping areas show predominantly low susceptibility values.

Several of the highly susceptible sectors are located upslope of the SS51 Alemagna road corridor, highlighting the potential interaction between debris-flow source areas and critical infrastructure along the valley. Although the present analysis focuses exclusively on the predisposition component, the resulting susceptibility map provides a first-order identification of areas where debris-flow processes are more likely to occur.

These results represent a fundamental step for the Alemagna Demonstration Case, supporting the identification of critical sectors along the corridor and providing a spatial framework for future analyses and risk mitigation strategies within the RETURN project.

7. Protocols for Ground Instabilities Mitigation

This chapter describes the mitigation strategies and the integration of real-time monitoring and Early Warning Systems (EWS) defined for the three Demonstration Cases (DCs) of the RETURN project. The contents are fully consistent with the framework, terminology and operational categories adopted in DV2.5.1, where mitigation measures are organised into:

- **Preventive measures** (reducing the likelihood of initiation)
- **Protective measures** (reducing the consequences of events)
- **Structural interventions**
- **Non-structural interventions**
- **Hybrid/combined solutions**
- **Monitoring strategies and EWS protocols**

The measures presented here are tailored to the instability scenarios identified through the RETURN toolchains (STONE, Parsifal, KATABASIS, RASH3D) and adapted to the morphological, geological and infrastructural characteristics of each DC. A summary of the mitigation and monitoring strategies for the DCs is reported in Table 7 at the end of this section.

7.1. Mitigation strategies scenarios for the Demonstration Cases

Mitigation strategies were derived by integrating:

(i) the spatial patterns of instability highlighted by the modelling toolchains;
(ii) the geomorphological and geological constraints of each DC;
(iii) the exposure of strategic assets such as railways, road networks and urbanised areas.

The following subsections summarise, for each DC, the most suitable combination of *preventive*, *protective*, *structural* and *non-structural* measures, following the DV2.5.1 taxonomy.

City of Naples Demonstration Case – Sinkholes

Sinkholes in Naples are predominantly associated with man-made cavities, leakage from ageing water and sewer networks, and subsurface instability affecting the urban fabric. Mitigation relies primarily on preventive and structural actions.

Preventive measures

- Systematic inspection and condition assessment of underground utilities (pressure/flow monitoring, leak-detection systems).
- Regular geophysical surveys (GPR, ERT, microgravity) to detect voids and weakened zones.
- Continuous satellite monitoring using Differential Interferometry SAR (DInSAR) to assess structural settlements.
- Updating and harmonising existing subsurface cavity databases.

Structural measures

- Stabilisation and filling of sub-surface cavities using cementitious or low-viscosity grouts.
- Reinforcement of weakened tuffaceous layers through anchors, meshes or sprayed concrete.
- Renewal or re-lining of obsolete pipelines to avoid leakage-driven subsidence.

Non-structural measures

- Urban load management in high-susceptibility zones.
- Land-use regulations to limit excavation and heavy construction in critical areas.
- Continuous satellite monitoring using Differential Interferometry SAR (DInSAR) to assess structural settlements.

- Definition of municipal alert zones for emergency planning.

City of Naples Demonstration Case – Debris flow in the Camaldoli hill

Parsifal simulations indicated slope failure under wet and seismic triggering, caused by the mechanical behaviour of volcanic and volcaniclastic soils.

Preventive measures

- Improvement of surface and subsurface drainage to reduce soil saturation.
- Vegetation management to enhance root reinforcement and reduce erosion.

Protective/Structural measures

- Construction or reinforcement of check dams and debris-retention basins in the main gullies.
- Installation of diversion channels or controlled outlets to reduce flow energy near urban areas.
- Local slope regrading or buttressing in the most unstable sectors.

Non-structural measures

- Maintenance schedules for existing hydraulic works.
- Delineation of hazard-prone corridors for civil protection planning.

Calabria Demonstration Case – Rockfall

STONE simulations for the coastal escarpment highlighted a critical central sector where trajectories may *potentially reach or intersect* the railway alignment.

Preventive measures

- Scaling and removal of detached or partially detached blocks.
- Surface and subsurface drainage improvements to reduce weathering and instability.

Protective/Structural measures

- High-energy rockfall barriers in the most exposed railway sections.
- Wire-mesh drapery systems, rock bolts and anchors on steep rock faces.
- Construction of protection berms or reinforced embankments near tunnel portals.

Non-structural measures

- Scheduled inspections of rock faces through terrestrial LiDAR or photogrammetry.
- Monitoring using radar technologies to assess the movement of blocks.
- Monitoring through the acquisition of optical images for real-time assessment of movements (i.e. Photomonitoring)
- Maintenance of protective works and periodic clearing of debris.
- Temporary traffic-management protocols during severe weather or alerts.

Calabria Demonstration Case – Debris flow in Fuscaldo area

Parsifal-based scenarios show slope instability at the headwater and transition zones of the Maddalena catchment.

Preventive measures

- Slope drainage enhancement to reduce saturation in thick colluvial deposits.
- Management of hillside vegetation and removal of excess loose material.

Protective/Structural measures

- Construction of selective and storage check dams in the upper channels.
- Sediment traps and retention basins upstream of inhabited areas.
- Channel rehabilitation and hydraulic corrections to improve conveyance.

Non-structural measures

- Scheduled maintenance of hydraulic structures and sediment removal.

- Identification of priority intervention zones for municipal risk planning.

Alemagna Demonstration Case – Debris flow

In the alpine setting of the Alemagna corridor, KATABASIS simulations identified predisposed slope units contributing to debris-flow channels.

Preventive measures

- Sediment management and regular cleaning of headwater channels.
- Vegetation control to limit obstruction and reduce sediment supply.

Protective/Structural measures

- Check dams, debris racks and deflection walls at channel outlets.
- Reinforced retaining structures and gabions protecting road segments.
- Energy-dissipation structures in steep reaches.

Non-structural measures

- Local rainfall-threshold calibration for rapid-onset debris flows.
- Land-use restrictions near alluvial fans and depositional areas.

7.2. Integration of real-time monitoring and early warning systems

The RETURN approach emphasises the integration of real-time monitoring networks, multi-sensor platforms, and threshold-based Early Warning Systems, following the criteria reported in DV2.5.1.

Monitoring strategies are structured into the following categories:

- **In-situ geotechnical sensors:** inclinometers, piezometers, TDR, strain gauges
- **Hydrological sensors:** rainfall intensity gauges, soil moisture probes, flow-level sensors
- **Remote sensing technologies:** satellite radar technology, ground-based radar, terrestrial LiDAR, optical monitoring
- **Process-specific detection systems:** geophones, vibro-acoustic sensors (debris flows), impact sensors (rockfall)
- **Integrated Early Warning Systems:** multi-threshold protocols, automated data acquisition, communication to stakeholders

Below, systems are customised for each DC.

City of Naples Demonstration Case

Sinkholes

- Distributed pressure/flow sensors for leak detection in water and sewer networks.
- Repeated geophysical surveys (ERT, GPR) for cavity detection.
- Differential Interferometry SAR for settlements' assessment.
- Settlement and deformation sensing in areas with known underground voids.

Debris flow

- Rainfall and soil-moisture stations supporting Parsifal-triggering thresholds.
- Ground-based radar or LiDAR for detecting shallow movements.
- Local EWS protocols based on hydrological conditions and forecasted rainfall.

Calabria Demonstration Case

Rockfall

- Ground-based interferometric radar (GB-InSAR) for continuous monitoring of unstable rock walls.
- Periodic LiDAR scans for change detection and volumetric assessment.
- Impact or vibration sensors along railway infrastructures.

- Automated warning protocols for railway operators.

Debris flow

- High-frequency rain gauges in the Maddalena basin.
- Geophones and vibro-acoustic sensors along the channel.
- Level sensors at fan apex locations.
- EWS thresholds derived from Parsifal outputs.

Alemagna Demonstration Case

Debris flow

- High-resolution rainfall monitoring for alpine trigger thresholds.
- Geophones for debris-flow front detection.
- Doppler radar or vibro-acoustic detection systems in steep tributary channels.
- Integrated EWS for coordination between ANAS and local civil protection.

Table 7 - Summary table of the mitigation and monitoring strategies for the DCs.

Demonstration Case	Ground Instability	Key scenario results	Recommended mitigation (DV2.5.1 categories)	Monitoring & EWS integration
City of Naples	Anthropogenic sinkholes	Localised subsurface voids, leakage-driven failures	*Preventive:* utility inspection, cavity mapping; *Structural:* grouting, reinforcement	Leak-detection sensors, geophysics, deformation monitoring
	Debris flow	Failures under high saturation / seismic loading	*Structural:* check dams, basins; *Preventive:* drainage; *Non-structural:* land-use rules	Rain/soil sensors, radar/LiDAR, threshold-based EWS
Calabria	Rockfall	Central sector potentially interacting with railway	*Protective:* barriers, drapery; *Preventive:* scaling; *Structural:* anchors	GB-InSAR, LiDAR, vibration sensors, railway-alert protocols
	Debris flow	Instability in headwaters and transition slopes	*Structural:* check dams, sediment traps; *Preventive:* slope drainage	Rain gauges, geophones, level sensors, Parsifal-based EWS
Alemagna	Debris flow	High susceptibility in tributary catchments	*Structural:* check dams, deflection structures; *Preventive:* sediment management	Rainfall monitoring, geophones, Doppler radar, integrated EWS

8. Conclusions

The activities carried out within Task 2.5.3 have demonstrated the operational applicability of the RETURN toolchains for assessing different types of Ground Instabilities (GIs) across heterogeneous geomorphological and infrastructural contexts. The three Demonstration Cases—City of Naples, Calabria and Alemagna—served as representative environments to verify the robustness, versatility and scalability of the modelling framework when confronted with real-world conditions.

A major outcome concerns the flexibility of the toolchains, which effectively adapted to settings ranging from urban environments affected by anthropogenic sinkholes and debris flows to coastal slopes and railway corridors exposed to rockfalls, and to alpine catchments prone to debris-flow processes. This adaptability confirms the capacity of the RETURN framework to provide consistent GI scenarios while accommodating diverse data availability, landscape configurations, and triggering mechanisms.

The toolchains also proved capable of integrating hydrological and seismic triggers, enabling the construction of multi-trigger scenarios that capture the combined effects of rainfall-induced pore-pressure increases, soil saturation dynamics and, where relevant, seismic accelerations. For selected processes, such as debris-flow and rockfall propagation, dynamic simulations offered additional insight into runout patterns and potential impacts on strategically exposed infrastructures.

The derivation of mitigation strategies, structured according to the preventive, protective, structural and non-structural categories defined in DV2.5.1, demonstrated the direct operational value of the modelling outputs. These strategies align with the physical processes highlighted by the simulations and with the requirements and constraints of the infrastructural systems present in the DCs. Their formulation has been further reinforced by continuous interaction with Transversal Spokes, which ensured methodological coherence, and by the contribution of stakeholders such as the Gruppo Ferrovie dello Stato (FS) and ANAS, who provided essential datasets, site-specific information and indications on priority corridors and areas requiring detailed assessment.

Despite these strengths, some limitations remain. Certain GI types are not yet fully represented due to incomplete tool validation or insufficiently detailed data. The modelling of preparatory processes and the explicit representation of multi-trigger interactions still require further refinement. These aspects indicate the need for continued development of the tools, the expansion of data integration capabilities and a stronger coupling between modelling components and real-time monitoring infrastructures.

In summary, the operational implementation conducted in Task 2.5.3 confirms the value of the RETURN toolchains as an effective and scalable framework for multi-hazard ground-instability assessment. The results highlight clear pathways for future enhancements aimed at improving model performance, supporting decision-making processes and strengthening the integration of the toolchains into stakeholder-driven workflows for risk mitigation and territorial resilience.

9. References

Alvioli, M., De Matteo, A., Castaldo, R., Tizzani, P., Reichenbach, P., 2022. Three-dimensional simulations of rockfalls in Ischia, Southern Italy, and preliminary susceptibility zonation. Geomatics, Natural Hazards and Risk 13, 2712–2736. https://doi.org/10.1080/19475705.2022.2131472

Beven, K.J., Lamb, R., Quinn, P., Romanowicz, R., Freer, J., 1995. TOPMODEL, in: Computer Models of Watershed Hydrology. Water Resources Publications, Colorado, pp. 627–668.

Bonardi, G., Cavazza, W., Perrone, V., Rossi, S., 2001. Calabria-Peloritani terrane and northern Ionian Sea, in: Vai, G.B., Martini, I.P. (Eds.), Anatomy of an Orogen: The Apennines and Adjacent Mediterranean Basins. Springer Netherlands, Dordrecht, pp. 287–306. https://doi.org/10.1007/978-94-015-9829-3_17

Borgatti, L., Soldati, M., 2010. Landslides as a geomorphological proxy for climate change: A record from the Dolomites (northern Italy). Geomorphology, Landslide geomorphology in a changing environment 120, 56–64. https://doi.org/10.1016/j.geomorph.2009.09.015

Breiman, L., 2001. Random Forests. Machine Learning 45, 5–32. https://doi.org/10.1023/A:1010933404324

Calcaterra, D., Coppin, D., de Vita, S., Di Vito, M.A., Orsi, G., Palma, B., Parise, M., 2007. Slope processes in weathered volcaniclastic deposits within the city of Naples: The Camaldoli Hill case. Geomorphology 87, 132–157. https://doi.org/10.1016/j.geomorph.2006.03.040

Cianflone, G., Larosa, S., Beccaro, L., Viscomi, A., Tolomei, C., Chiodo, G., La Pietra, T., Leonetti, S., Mollica, L., Pellegrino, A., Servidio, A., Siviglia, S., Imbrogno, G., Ietto, F., Dominici, R., 2025. A revised landslide inventory of the Calabria Region (Italy). Journal of Maps 21, 2421292. https://doi.org/10.1080/17445647.2024.2421292

Claps, P., Evangelista, G., Ganora, D., Mazzoglio, P., Monforte, I., 2024. FOCA: a new quality-controlled database of floods and catchment descriptors in Italy. Earth System Science Data 16, 1503–1522. https://doi.org/10.5194/essd-16-1503-2024

De Vivo, B., Rolandi, G., Gans, P.B., Calvert, A., Bohrson, W.A., Spera, F.J., Belkin, H.E., 2001. New constraints on the pyroclastic eruptive history of the Campanian volcanic Plain (Italy). Mineralogy and Petrology 73, 47–65. https://doi.org/10.1007/s007100170010

Deganutti, A.M., Tecca, P., 2013. The Case Study of Cancia (Dolomites, Italy), a Mountain Village Threatened by a Debris Flow, in: Margottini, C., Canuti, P., Sassa, K. (Eds.), Landslide Science and Practice: Volume 6: Risk Assessment, Management and Mitigation. Springer, Berlin, Heidelberg, pp. 329–333. https://doi.org/10.1007/978-3-642-31319-6_44

Esposito, C., Martino, S., Pallone, F., Martini, G., Romeo, R.W., 2016. A methodology for a comprehensive assessment of earthquake-induced landslide hazard, with an application to pilot sites in Central Italy, in: Landslides and Engineered Slopes. Experience, Theory and Practice. CRC Press.

Evangelista, A., Scotto di Santolo, A., 2004. Analysis and Field Monitoring of Slope Stability in Unsaturated Pyroclastic Soil Slopes in Napoli, Italy. International Conference on Case Histories in Geotechnical Engineering.

Fawcett, T., 2006. An introduction to ROC analysis. Pattern Recognition Letters, ROC Analysis in Pattern Recognition 27, 861–874. https://doi.org/10.1016/j.patrec.2005.10.010

Ferrarotti, M., 2026. Role of wildfires and snow covers as preparatory factors in multi-hazard shallow landslide scenarios through ml emulators (PhD Thesis). Sapienza University of Rome.

Filice, F., Liberi, F., Cirillo, D., Pandolfi, L., Marroni, M., Piluso, E., 2015. Geology map of the central area of Catena Costiera: insights into the tectono-metamorphic evolution of the Alpine belt in Northern Calabria. Journal of Maps 11, 114–125. https://doi.org/10.1080/17445647.2014.944877

Friedman, J.H., 2001. Greedy function approximation: A gradient boosting machine. The Annals of Statistics 29, 1189–1232. https://doi.org/10.1214/aos/1013203451

Fusco, F., De Vita, P., Mirus, B.B., Baum, R.L., Allocca, V., Tufano, R., Di Clemente, E., Calcaterra, D., 2019. Physically Based Estimation of Rainfall Thresholds Triggering Shallow Landslides in Volcanic Slopes of Southern Italy. Water 11, 1915. https://doi.org/10.3390/w11091915

Fusco, F., Tufano, R., De Vita, P., Di Martire, D., Di Napoli, M., Guerriero, L., Mileti, F.A., Terribile, F., Calcaterra, D., 2023. A revised landslide inventory of the Campania region (Italy). Sci Data 10, 355. https://doi.org/10.1038/s41597-023-02155-6

Guarino, P.M., Nisio, S., 2012. Anthropogenic sinkholes in the territory of the city of Naples (Southern Italy). Physics and Chemistry of the Earth, Parts A/B/C, Innovative modelling approaches for disaster risk reduction 49, 92–102. https://doi.org/10.1016/j.pce.2011.10.023

Guzzetti, F., Crosta, G., Detti, R., Agliardi, F., 2002. STONE: a computer program for the three-dimensional simulation of rock-falls. Computers & Geosciences 28, 1079–1093. https://doi.org/10.1016/S0098-3004(02)00025-0

Hofierka, J., Mitášová, H., Neteler, M., 2009. Chapter 17 Geomorphometry in GRASS GIS, in: Developments in Soil Science. Elsevier, pp. 387–410. https://doi.org/10.1016/S0166-2481(08)00017-2

ISPRA, 2007. Note Illustrative della Carta geologica d'Italia alla scala 1:50.000, F. 029 Cortina d'Ampezzo. ISPRA - Serv. Geol. d'It., Roma.

James, G., Witten, D., Hastie, T., Tibshirani, R., 2021. An Introduction to Statistical Learning: with Applications in R, Springer Texts in Statistics. Springer US, New York, NY. https://doi.org/10.1007/978-1-0716-1418-1

Nelder, J.A., Wedderburn, R.W.M., 1972. Generalized Linear Models. Journal of the Royal Statistical Society. Series A (General) 135, 370–384. https://doi.org/10.2307/2344614

Panizza, M., Pasuto, A., Silvano, S., Soldati, M., 1996. Temporal occurrence and activity of landslides in the area of Cortina d'Ampezzo (Dolomites, Italy). Geomorphology, Landslides in the European Union 15, 311–326. https://doi.org/10.1016/0169-555X(95)00077-I

Parise, M., 2015. A procedure for evaluating the susceptibility to natural and anthropogenic sinkholes. Georisk: Assessment and Management of Risk for Engineered Systems and Geohazards 9, 272–285. https://doi.org/10.1080/17499518.2015.1045002

Pirulli, M., Bristeau, M.-O., Mangeney, A., Scavia, C., 2007. The effect of the earth pressure coefficients on the runout of granular material. Environmental Modelling & Software, Modelling, computer-assisted simulations, and mapping of dangerous phenomena for hazard assessment 22, 1437–1454. https://doi.org/10.1016/j.envsoft.2006.06.006

Pokharel, B., Lim, S., Bhattarai, T.N., Alvioli, M., 2023. Rockfall susceptibility along Pasang Lhamu and Galchhi-Rasuwagadhi highways, Rasuwa, Central Nepal. Bull Eng Geol Environ 82, 183. https://doi.org/10.1007/s10064-023-03174-8

Robustelli, G., Muto, F., Scarciglia, F., Spina, V., Critelli, S., 2005. Eustatic and tectonic control on Late Quaternary alluvial fans along the Tyrrhenian Sea coast of Calabria (South Italy). Quaternary Science Reviews, Quaternary coastal morphology and sea-level changes 24, 2101–2119. https://doi.org/10.1016/j.quascirev.2004.08.025

Santangelo, M., Alvioli, M., Baldo, M., Cardinali, M., Giordan, D., Guzzetti, F., Marchesini, I., Reichenbach, P., 2019. Brief communication: Remotely piloted aircraft systems for rapid emergency response: road exposure to rockfall in Villanova di Accumoli (central Italy). Natural Hazards and Earth System Sciences 19, 325–335. https://doi.org/10.5194/nhess-19-325-2019

Scarpati, C., Perrotta, A., Lepore, S., Calvert, A., 2012. Eruptive history of Neapolitan volcanoes: constraints from 40Ar–39Ar dating. Geological Magazine 150, 412–425. https://doi.org/10.1017/S0016756812000854

Schmidt, K.M., Roering, J.J., Stock, J.D., Dietrich, W.E., Montgomery, D.R., Schaub, T., 2001. The variability of root cohesion as an influence on shallow landslide susceptibility in the Oregon Coast Range. Can. Geotech. J. 38, 995–1024. https://doi.org/10.1139/t01-031

Sorriso-Valvo, M., Sylvester, A.G., 1993. The relationship between geology and landforms along a coastal mountain front, northern Calabria, Italy. Earth Surface Processes and Landforms 18, 257–273. https://doi.org/10.1002/esp.3290180307

Tufano, R., Guerriero, L., Annibali Corona, M., Bausilio, G., Di Martire, D., Nisio, S., Calcaterra, D., 2022. Anthropogenic sinkholes of the city of Naples, Italy: an update. Nat Hazards 112, 2577–2608. https://doi.org/10.1007/s11069-022-05279-x

Van Westen, C. J., 1993. Application of Geographic Information Systems to Landslide Hazard Zonation, *Ph-D Dissertation* Technical University Delft. ITC-Publication Number 15, ITC, Enschede, The Netherlands, 245 pp.